

Fall 12-18-2020

## Outcomes of Unilateral Alveolar Clefts Grafted Using Recombinant Human Bone Morphogenetic Protein-2: A Retrospective Volumetric Analysis Using CBCT

Landon Robert Peterson  
*University of Nebraska Medical Center*

Tell us how you used this information in this [short survey](#).

Follow this and additional works at: <https://digitalcommons.unmc.edu/etd>



Part of the [Oral and Maxillofacial Surgery Commons](#), and the [Orthodontics and Orthodontology Commons](#)

---

### Recommended Citation

Peterson, Landon Robert, "Outcomes of Unilateral Alveolar Clefts Grafted Using Recombinant Human Bone Morphogenetic Protein-2: A Retrospective Volumetric Analysis Using CBCT" (2020). *Theses & Dissertations*. 503.

<https://digitalcommons.unmc.edu/etd/503>

This Thesis is brought to you for free and open access by the Graduate Studies at DigitalCommons@UNMC. It has been accepted for inclusion in Theses & Dissertations by an authorized administrator of DigitalCommons@UNMC. For more information, please contact [digitalcommons@unmc.edu](mailto:digitalcommons@unmc.edu).

**OUTCOMES OF UNILATERAL ALVEOLAR CLEFTS GRAFTED USING  
RECOMBINANT HUMAN BONE MORPHOGENETIC PROTEIN-2: A  
RETROSPECTIVE VOLUMETRIC ANALYSIS USING CBCT**

By

**Landon Robert Peterson**

A THESIS

Presented to the Faculty of  
the University of Nebraska Graduate College  
in Partial Fulfillment of Requirements  
for the Degree of Master of Science

Medical Sciences Interdepartmental Area Graduate Program  
(Oral Biology)

Under the Supervision of  
Professor Sundaralingam (Prem) Premaraj, B.D.S., M.S., Ph.D., FRCD(C)

University of Nebraska Medical Center  
Omaha, Nebraska

December, 2020

Advisory Committee:

Valmont P. Desa, D.D.S., M.D., FACS

Peter J. Giannini, D.D.S., M.S.

Sung K. Kim, D.D.S. (ex officio)

Gregory G. Oakley, Ph.D.

## ACKNOWLEDGMENTS

I would like to begin by thanking my advisory chair, Dr. Sundaralingam Premaraj, for his mentorship, expertise on this subject matter, continued guidance, and overall friendship throughout this process. You were available when needed and assisted me in finding previous literature articles relating to this project. Your willingness to help was appreciated throughout this endeavor including thesis project ideas, IRB submission, and thesis revisions. I will forever be grateful to have learned and worked under your supervision to achieve this master's degree.

Next, I would like to thank the other members of my advisory committee. Thank you Dr. Desa for your time, wisdom, and assistance during the data retrieval process. Thank you Dr. Giannini for your assistance with IRB submissions and thesis edits. Thank you Dr. Kim for your guidance on the volumetric software and expertise on radiographic analysis. Thank you Dr. Oakley for structuring annual presentation seminars and overall support. This thesis project could not have been completed successfully without the numerous contributions from each of you.

Furthermore, there are many other people that have assisted with this project and I feel they need to be recognized. Thank you Dr. Kolb and the Boys Town team for your assistance with the Boys Town IRB submission process. Sunit Patel, many thanks for your hard work and dedication with radiographic analysis. A huge thank you to Emily Robinson for your wonderful work with statistical analysis, interpretation, and graph development. Thank you to Kim Theesen for helping create several of the images included in this thesis. Without the aid of all of you, this project would not have been a success.

Last but certainly not least, I would like to thank my family. To my wife, Katelyn, I love you greatly. Thank you for your endless support and for always pushing me to be my best. Mom and Dad, words will never be enough. Your continuous sacrifices and demonstration of love continue to motivate me on a daily basis. Thank you to my sisters for always showing support throughout my educational journey. I hope I have made you proud. I love you all greatly.

**OUTCOMES OF UNILATERAL ALVEOLAR CLEFTS GRAFTED USING  
RECOMBINANT HUMAN BONE MORPHOGENETIC PROTEIN-2: A  
RETROSPECTIVE VOLUMETRIC ANALYSIS USING CBCT**

Landon R. Peterson, M.S.

University of Nebraska, 2020

Advisor: Sundaralingam Premaraj, B.D.S., M.S., Ph.D., FRCD(C)

Purpose of this study is to evaluate the success rates of secondary alveolar grafts using recombinant human bone morphogenetic protein with CBCT and to evaluate the effects of several variables on these outcomes. After our inclusion/exclusion criteria, records of 24 patients receiving secondary alveolar grafts at the University of Nebraska Medical Center were evaluated. Pre-graft and 6-month post-graft cleft volumes were measured using ITK-SNAP 3.8.0 software to determine a percent residual defect following surgery. Of the 24 patients, one was excluded as the graft surgery was deemed a failure. The patients' gender, age, side of cleft, cleft side canine root lengths, angulations, and distance from the occlusal plane were also measured. The mean volumetric values for the pre-graft and post-graft clefts were 1049.30mm<sup>3</sup> and 413.75mm<sup>3</sup>, respectively with a mean residual defect value of 0.32 (SD = 0.22). The difference in percent residual defect following the graft was not statistically significant for any of the variables measured, except for gender (F=10.63; DF=1,21; p=0.0037). This study showed females undergoing secondary grafts of unilateral alveolar clefts have a lower percent residual defect six months following surgery. However, the results of this study may not represent clinical outcomes and larger sample sizes may be helpful to conclude statistically significant differences between our variables.

## TABLE OF CONTENTS

ACKNOWLEDGEMENTS.....	i
ABSTRACT.....	ii
TABLE OF CONTENTS.....	iii
LIST OF FIGURES.....	vi
LIST OF TABLES.....	viii
CHAPTER 1: INTRODUCTION.....	1
CHAPTER 2: LITERATURE REVIEW.....	5
2.1. Cleft Lip and Cleft Palate .....	5
2.1.1. Etiology.....	5
2.1.2. Biological Considerations .....	6
2.1.3. Associated Syndromes.....	7
2.1.4. Classification.....	9
2.1.5. Prevalence.....	10
2.2. Alveolar Cleft.....	11
2.3. Managing Alveolar Clefts.....	12
2.3.1. History.....	12
2.3.2. Goals.....	13
2.3.3. Treatment Timing.....	13
2.3.4. Outcomes and Success Rates.....	14
2.4. Materials Used for Secondary Alveolar Grafts.....	17
2.5. Cone Beam Computed Tomography to Evaluate Alveolar Graft Procedures.....	21
CHAPTER 3: RESEARCH HYPOTHESIS & SPECIFIC AIMS .....	23
3.1. Statement of the Problem.....	23

3.2. Central Research Hypothesis .....	24
3.3. Specific Aims.....	24
CHAPTER 4: MATERIALS & METHODS.....	25
4.1. Study Design.....	25
4.1.1. Data Collection.....	25
4.1.2. Surgical Technique.....	26
4.2. Linear Measurements.....	27
4.3. Volumetric Measurements.....	29
4.4. Statistical Analysis.....	31
4.5. Intra-examiner and Inter-examiner Reliability.....	32
CHAPTER 5: RESULTS.....	49
5.1. Subjects.....	49
5.2. Demographic Variables and Their Effects on Outcomes.....	49
5.2.1. Gender.....	49
5.2.2. Age of the Patient at the Time of Grafting .....	50
5.2.3. Side of the Alveolar Cleft .....	50
5.3. Linear Values and Their Effects on Outcomes.....	51
5.3.1. Cleft Side Canine Root Length.....	51
5.3.2. Cleft Side Canine Angulation; Coronal Section.....	51
5.3.3. Cleft Side Canine Angulation; Sagittal Section.....	52
5.3.4 Cleft Side Canine Distance from the Occlusal Plane.....	53
5.4. Volumetric Values and Percent Residual Defect.....	53
5.5. Intra-examiner and Inter-examiner Reliability.....	54

CHAPTER 6: DISCUSSION.....	80
6.1. Demographic Variables and Their Effects on Outcomes.....	80
6.1.1. Gender.....	80
6.1.2. Age of the Patient at the Time of Grafting.....	80
6.1.3. Side of the Alveolar Cleft.....	81
6.2. Linear Values and Their Effects on Outcomes.....	81
6.2.1. Cleft Side Canine Root Length.....	81
6.2.2. Cleft Side Canine Angulation; Coronal and Sagittal Sections.....	82
6.2.3. Cleft Side Canine Distance from the Occlusal Plane.....	83
6.3. Volumetric Values and Percent Residual Defect.....	84
6.4. Limitations of the Study.....	85
6.4.1. Radiographic Limitations.....	85
6.4.2. Software Limitations.....	86
6.4.3. Sample Limitations.....	87
6.5. Conclusions.....	87
6.6. Future Research.....	88
BIBLIOGRAPHY.....	90

## LIST OF FIGURES

Figure 1.1. Unilateral Alveolar Cleft.....	4
Figure 2.1.1. Normal Embryologic Development.....	33
Figure 2.1.4. Kernahan Striped “Y” Classification System.....	34
Figure 2.2.1. Alveolar Cleft Shape.....	35
Figure 2.5.1. Bergland Scale.....	36
Figure 2.5.2. Chelsea Scale.....	37
Figure 4.2.1. Cleft Side Canine Root Length Measurement.....	38
Figure 4.2.2. Cleft Side Canine Angulation; Coronal Section.....	39
Figure 4.2.3. Cleft Side Canine Angulation; Sagittal Section.....	40
Figure 4.3.1. Region of Interest for Semi-automatic Mode.....	41
Figure 4.3.2. Active Contour Evolution Parameters in ITK-SNAP 3.8.0.....	42
Figure 4.3.3. Pre-set Bubbles in the Initialization Mode.....	43
Figure 4.3.4. Auto-segmentation of Bone and/or Hard Tissues.....	44
Figure 4.3.5. Polygon Mode; Manual Segmentation of the Cleft.....	45
Figure 4.3.6. Final Volumetric Segmentation Image in ITK-SNAP 3.8.0.....	47
Figure 4.3.7. Final Volumetric Measurement in ITK-SNAP 3.8.0.....	48
Figure 5.2.1.1. Box & Whisker Plot for Male/Female.....	56
Figure 5.2.1.2. Least Squares Means Plot for Male/Female.....	58
Figure 5.2.2.1. Scatter Plot – Age of Patient at Time of Grafting.....	59
Figure 5.2.3.1. Box & Whisker Plot for Left/Right Side Alveolar Cleft.....	61
Figure 5.2.3.2. Least Squares Means Plot for Left/Right Side Alveolar Cleft.....	63
Figure 5.3.1.1. Scatter Plot – Cleft Side Canine Root Length.....	64
Figure 5.3.2.1. Scatter Plot – Cleft Side Canine Angulation (Coronal).....	66
Figure 5.3.3.1. Scatter Plot – Cleft Side Canine Angulation (Sagittal).....	68



Figure 5.3.4.1. Scatter Plot – Cleft Side Canine Distance from Occlusal Plane.....	70
Figure 5.4.1. Overall Volumetric Values for Unilateral Clefts.....	72
Figure 5.4.2. Percent Residual Defect Using rhBMP-2.....	73
Figure 5.4.3. Percent Residual Defect Using rhBMP-2; Male/Female.....	74
Figure 5.4.4. Percent Residual Defect Using rhBMP-2; Left/Right Alveolar Cleft.....	75

## LIST OF TABLES

Table 4.3.1. Region of Interest Boundaries for Manual Segmentation .....	46
Table 5.2.1.1. Type III Tests for Fixed Effects – Male/Female.....	57
Table 5.2.1.2. Least Squares Means – Male/Female.....	57
Table 5.2.2.1. Type I Tests of Fixed Effects - Age.....	60
Table 5.2.2.2. Regression Coefficient Estimates for Age of the Patient.....	60
Table 5.2.3.1. Type III Tests for Fixed Effects – Left/Right Side Alveolar Cleft.....	62
Table 5.2.3.2. Least Squares Means – Left/Right Side Alveolar Cleft.....	62
Table 5.3.1.1. Type I Tests of Fixed Effects – Cleft Side Canine Root Length.....	65
Table 5.3.1.2. Regression Coefficient Estimates for Cleft Side Canine Root Length.....	65
Table 5.3.2.1. Type I Tests of Fixed Effects – Cleft Side Canine Angulation (Coronal).....	67
Table 5.3.2.2. Regression Coefficient Estimates for Cleft Side Canine Angulation (Coronal).....	67
Table 5.3.3.1. Type I Tests of Fixed Effects – Cleft Side Canine Angulation (Sagittal).....	69
Table 5.3.3.2. Regression Coefficient Estimates for Cleft Side Canine Angulation (Sagittal).....	69
Table 5.3.4.1. Type I Tests of Fixed Effects – Cleft Side Canine Distance from Occlusal Plane.....	71
Table 5.3.4.2. Regression Coefficient Estimates for Cleft Side Canine Distance from Occlusal Plane.....	71
Table 5.4.1. Overall Volumetric Values for Unilateral Clefts.....	72
Table 5.4.2. Percent Residual Defect Using rhBMP-2.....	73
Table 5.5.1. Inter-examiner Reliability Raw Data.....	76
Table 5.5.2. Inter-examiner ICC3 Results.....	76
Table 5.5.3. Intra-examiner ICC3 Results for Cleft Volume; Investigator LP.....	77
Table 5.5.4. Intra-examiner ICC3 Results for Cleft Volume; Investigator SP.....	77

Table 5.5.5. Inter-examiner ICC3 Results for Cleft Side Canine Length.....	77
Table 5.5.6. Intra-examiner ICC3 Results for Cleft Side Canine Length; Investigator LP.....	78
Table 5.5.7. Intra-examiner ICC3 Results for Cleft Side Canine Length; Investigator SP.....	78
Table 5.5.8. Intra-examiner ICC3 Results for Cleft Side Canine Angulation (Coronal); Investigator LP.....	78
Table 5.5.9. Intra-examiner ICC3 Results for Cleft Side Canine Angulation (Sagittal); Investigator LP.....	79
Table 5.5.10. Intra-examiner ICC3 Results for Cleft Side Canine Distance from Occlusal Plane; Investigator LP.....	79

## CHAPTER 1: INTRODUCTION

Birth defects are always a concern for parents and may cause lifelong setbacks, especially in the early part of the child's life. In the United States, 7,500 children are born every year with orofacial clefts, and the lifetime medical cost per child with orofacial clefts is significant, averaging \$100,000 (Tolarová and Cervenka 1998). Worldwide, cleft lip and palate are among the most common birth defects that occur. These can occur as isolated conditions or they can be a component of a syndrome or inherited disease. The prevalence of cleft palate is 1 per 1,574 live births. The prevalence of cleft lip, with or without cleft palate, is 1 per 940 live births (Parker et al. 2010). Within this group of patients born with cleft lip and palate, approximately 75% have maxillary alveolar clefts (Bell et al. 1980).

According to Kang, an alveolar cleft is “a tornado-shaped bone defect in the maxillary arch” (2017). Alveolar clefts cause a disruption to the normal continuous bony environment in the maxillary arch. This can lead to multiple factors that affect the child and child's parents including: early feeding difficulties, nutritional issues, developmental delays, speech difficulties, facial asymmetry, hearing loss, discomfort during and/or following surgical procedures, time commitments, the need for orthodontic care, and possibly psychosocial issues for the child and/or child's parents (Coots 2012).

Bone grafting of alveolar clefts has become an essential component in the contemporary management of patients with orofacial clefts. Secondary alveolar bone grafting has been shown to improve some of the factors listed above as well as allow for successful orthodontic treatment and implant or prosthetic rehabilitation (Cho-Lee et al. 2013).

Up until about the past 10 years, anterior iliac crest (AIC) autogenic bone has been considered the gold standard grafting material for alveolar clefts. AIC's regeneration potential and high success rates make it a viable option for these children (Kazemi et al. 2002). However, there are several shortcomings with using iliac crest including: significant post-operative

morbidity, hematomas, pain, delayed ambulation, and prolonged hospitalization (Baqain et al. 2009). To overcome these shortcomings, there have been attempts to find a viable replacement material to use in secondary alveolar grafts. Recombinant human bone morphogenetic protein 2 (rhBMP-2) was approved by the Food and Drug Administration for maxillary sinus augmentation in 2004 and ridge augmentation following dental extractions in 2007. This material has since been shown to be a successful alternative when reconstructing an alveolar cleft (Francis et al. 2013; van Hout et al. 2011).

The proper timing for reconstructing alveolar clefts is still slightly controversial. Secondary alveolar bone grafting, undertaken late in mixed dentition before eruption of the canine, is currently considered the standard treatment (Francis et al. 2013). There are also a number of other variables that are believed to influence the outcome of alveolar bone grafts including: chronological age of the patient at the time of the graft, stage of root development for the cleft side canine at the time of the graft, the surgeon who performed the graft, and unilateral versus bilateral clefts (Francis et al. 2013; Oberoi et al. 2009; Seifeldin 2016). The way in which we view several of these variables has changed over time.

Occlusal and periapical radiographs have been used to evaluate bone fill within these alveolar clefts and to map segmentally the height, thickness, and position of bone on the roots adjacent to the cleft. Hammoudeh et al. reported the results of comparing rhBMP-2 with a demineralized bone matrix versus iliac crest bone for secondary alveolar bone graft using occlusal radiographs (2017). There are obvious shortcomings in attempting to determine the outcomes of alveolar bone grafts from 2-dimensional images. With the advent of 3-dimensional imaging systems such as cone beam computed tomography (CBCT), a more accurate analysis can be performed when studying alveolar bone graft outcomes. Thus, CBCT has become the new standard for analyzing bone fill of alveolar clefts.

The rationale for this project is that its successful completion would help to determine the effects of several variables on the proper timing of secondary alveolar graft procedures and on the success rates for these procedures. CBCT analysis of maxillary alveolar clefts allow for assessing the bone defect in three dimensions, a shortcoming of previous conventional radiographic studies. This research is potentially innovative because our specific variables and their effects on unilateral alveolar cleft grafting success rates have yet to be explored with 3-dimensional software in regards to these treatment differences. The primary impact of our anticipated findings would be determining the overall success rates of secondary alveolar grafting procedures using rhBMP-2 as an alternative material and understanding specific variables that may allow craniofacial and cleft teams to better manage patients with orofacial clefts.

The purpose of this study is to evaluate the success rates of secondary alveolar grafts using rhBMP-2 as a grafting material with 3-dimensional CBCT as well as to evaluate the effects of several variables on these outcomes.

The null hypothesis is there will be no difference in secondary alveolar graft success rates when comparing our specific variables and their effects on these outcomes using 3-dimensional software for analysis.

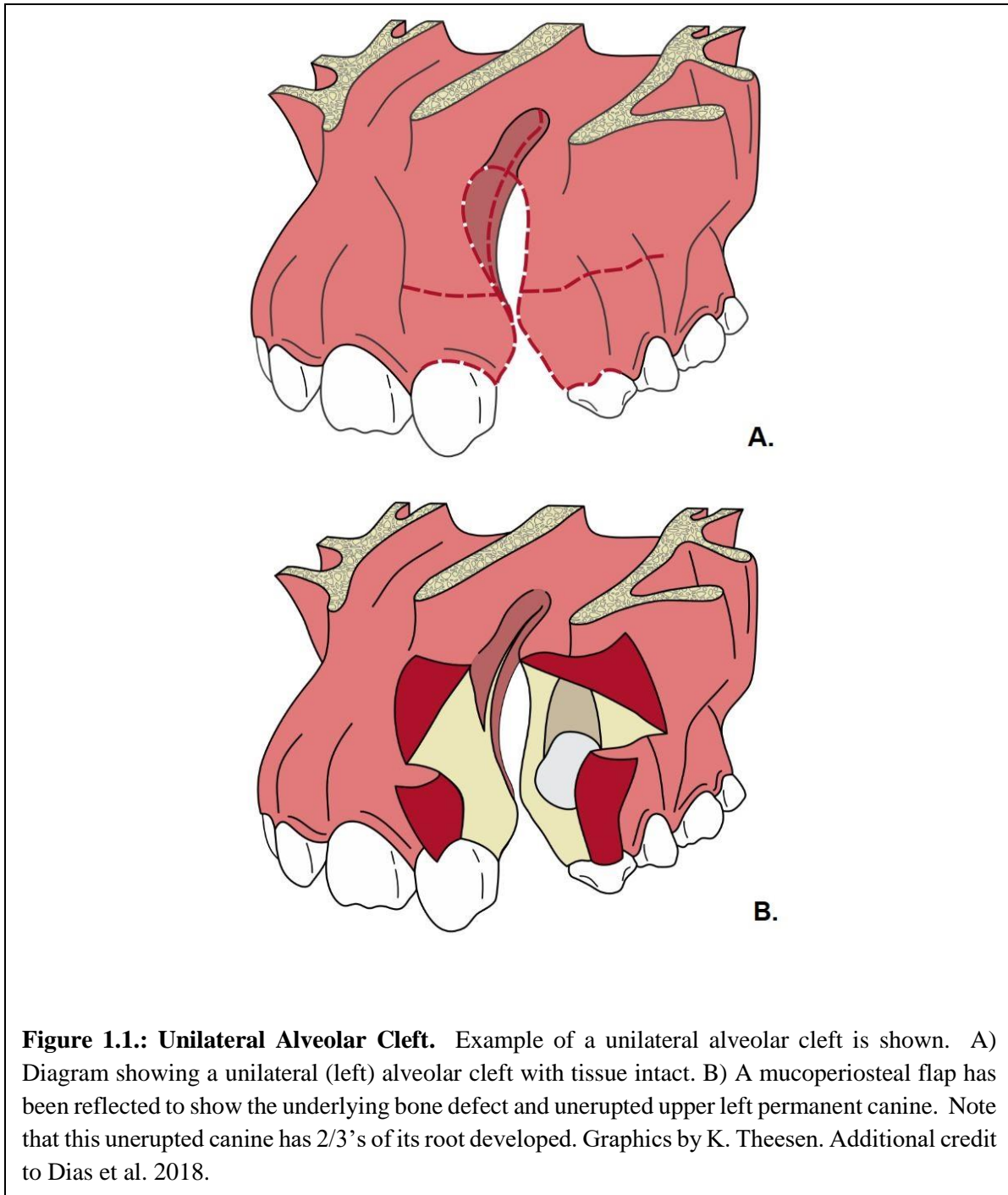


**Figure 1.1.: Unilateral Alveolar Cleft.** Example of a unilateral alveolar cleft is shown. A) Diagram showing a unilateral (left) alveolar cleft with tissue intact. B) A mucoperiosteal flap has been reflected to show the underlying bone defect and unerupted upper left permanent canine. Note that this unerupted canine has 2/3's of its root developed. Graphics by K. Theesen. Additional credit to Dias et al. 2018.

## CHAPTER 2: LITERATURE REVIEW

### 2.1. Cleft Lip and Cleft Palate

#### 2.1.1. Etiology

Development of cleft lip and cleft palate (CLCP) happens early in embryologic development. Between the fourth and eighth week of embryologic life, the embryo undergoes rapid changes in shape and growth as the six branchial arches are formed. The first two branchial arches are responsible for the development of the face and the cranium. The face begins to develop from the ectomesenchyme, derived from neural crest cells, which forms five prominences. These prominences include the frontonasal process and two maxillary and two mandibular processes (one of each per side) surrounding a central depression (Sperber et al. 2001).

The primary and secondary palates are derived from the medial nasal and maxillary processes and are two of the main structures involved with the formation of orofacial clefts. Rani et al. defines the primary palate as comprising the premaxilla, anterior septum, and upper lip. The roof of the mouth extends from the incisive foramen or its vestige, the incisive papilla, to the uvula. This area is termed the secondary palate. The incisive foramen is the dividing line between the primary and secondary palates (2011).

Clefting of the lip occurs in response to a failure of fusion between the medial nasal process, which is an extension of the frontonasal process, and the maxillary prominence. The fusion of these prominences normally occurs during the sixth week of embryologic development. The normal fusion of these structures during primary palate formation creates not only the upper lip but also the area of the alveolar ridge containing the central and lateral incisors. Since there is a disruption in the normal development of this area, a cleft in the alveolar process will often accompany a cleft lip (Proffit et al. 2013).



Clefting of the palate occurs in response to a slightly different abnormality. Closure of the secondary palate by elevation of the palatal shelves follows the formation of the primary palate by nearly two weeks; around the eighth week of embryologic life. There is a disruption in this normal fusion of the palatal shelves, which leads to a palatal cleft. An interference with normal lip closure that is still present at this time can also affect the proper development of the secondary palate. About 60% of subjects with cleft lip also have cleft palate (Proffit et al. 2013). Additionally, 75% of individuals born with cleft lip and palate have maxillary alveolar clefts (Bell et al. 1980).

Normal embryologic development (Figure 2.1.1) of other facial structures is also a result of proper fusion of prominences derived from the first two branchial arches. For example, the mandibular processes fuse to form the lower lip and jaw and the lateral nasal processes form the alar structure of the nose bilaterally (Sperber et al. 2001).

### **2.1.2. Biological Considerations**

As the neural crest cells migrate and proliferate to their respective branchial arches, they interact with extracellular matrix and adjacent epithelia, which partly determines the patterning and nature of the derivative tissues they will form. These include neural, skeletal, connective, and muscular tissues (Sarkar et al. 2001).

The development of facial structures is the result of cell proliferation, differentiation, adhesion, and apoptosis. The facial prominences of the neural crest cells are controlled by molecular signals. These signals are a result of interactions and responses to genes that include the transforming growth factor beta (TGF- $\beta$ ) super family, sonic hedgehog (SHH), fibroblast growth factors (FGFs), and bone morphogenic proteins (BMPs). Orofacial clefts are a result of failures or errors in any of these intracellular mechanisms that disrupt the normal fusion or development of facial prominences (Marazita and Mooney 2004).

In addition to the genes listed previously, there are a number of other genes that have been linked to orofacial cleft development. The homeobox (Hoxa-1, Hoxa-2, Hoxb-1, Hoxb-3, Hoxb-4), OXT (orthodontical), GSC (goosecoid), DLX (distalless), and MSX (muscle segment) gene families have also been expressed in the ectomesenchyme derived from the neural crest. Many of these genes are candidates for causing orofacial clefting (Sperber et al. 2001).

There are also environmental factors that contribute to the development of orofacial clefts. These factors can be divided into four groups: drugs, chemicals, maternal metabolic imbalances (folic acid deficiency), and maternal infections. Maternal consumption of alcohol and teratogenic medications such as retinoids, corticosteroids, and anti-convulsants during the periconceptional period can cause facial abnormalities including orofacial clefts (Eppley et al. 2005). Genetic mutations and environmental impacts upon the complex mechanisms of craniofacial development lead to phenotypic anomalies, of which orofacial clefting is the most common (Schutte and Murray 1999).

Many mechanisms underlying normal and abnormal embryogenesis of the craniofacial structures are well understood. The genetic factors that cause abnormal development and result in orofacial clefts are not completely clear, however much progress has been accomplished over the years. The emerging consensus is that the genetic etiology of nonsyndromic clefting is complex, with several loci showing drastic results in at least some studies. In addition, genes or chromosomal rearrangements on many chromosomes can lead to syndromes that include orofacial clefts (Marazita and Mooney 2004).

### **2.1.3. Associated Syndromes**

As we have learned, orofacial clefts can have an environmental or genetic origin depending on how the abnormality was caused. Although the nonsyndromic clefts are more common and likely due to secondary gene-environment interactions, orofacial clefts can occur as one component of multiple congenital anomaly syndromes (Schutte and Murray 1999).

Every structural abnormality in the body that is congenital represents an embryologic error in morphogenesis and may affect one or more systems (Venkatesh 2009). There are currently over 400 known syndromes either directly or indirectly associated with cleft lip and/or cleft palate. It has been estimated that approximately three percent of all orofacial cleft cases are related to known syndromes (Fraser 1970).

Van der Woude syndrome is one of the most common syndromes associated with orofacial clefts. This syndrome is autosomal dominant and can display several other features including: hypodontia, missing maxillary or mandibular second premolar teeth, absent maxillary lateral incisor, ankyloglosia, and the hallmark feature of lower lip pits (Venkatesh 2009).

Another autosomal dominant disorder that is associated with orofacial clefts is Treacher Collins syndrome. This syndrome results from the loss-of-function mutation in the TCOF-1 gene. This gene encodes for the phosphoprotein “treacle” and can affect craniofacial development. Treacher Collins syndrome affects the size and shape of the ears, cheekbones, and jaw. Some of the key features include: downslanting eyes, underdeveloped cheek and jaw bones, notched lower eyelids, and cleft palate (Dixon et al. 2000).

Pierre Robin sequence is another congenital condition that is associated with cleft lip and/or cleft palate. In 1926, Pierre Robin published a case with a triad of glossoptosis, micrognathia, and airway obstruction. Although cleft palate was not included in this triad, they are frequently associated with this sequence. The most accepted theory involves the initial event of mandibular hypoplasia, which keeps the tongue elevated in the oral cavity. This prevents fusion of the palatal shelves resulting in cleft palate (Venkatesh 2009).

Velocardiofacial syndrome is another autosomal dominant condition that is associated with orofacial clefts. This syndrome is a result of a sub-microscopic deletion on the long arm of chromosome 22 in the “q11” region. It was first described by Dr. Robert Shprintzen and affects every major system in the body. Some of the more common features include: cleft palate, minor learning problems, speech issues, feeding problems, and cardiac anomalies (Venkatesh 2009)

Stickler syndrome is a connective tissue disorder that is also associated with cleft palate. It is also an autosomal dominant disorder with ophthalmological and orofacial features. Stickler syndrome is a result of a mutation in the COL2A1 gene and children with this condition can display midline clefting ranging in severity from a cleft of the soft palate to complete cleft lip and palate. Other features of this syndrome include: a flat midface with depressed nasal bridge, short nose, anteverted nares, and micrognathia (Snead and Yates 1999).

Understanding the etiology of orofacial clefts is vital for proper prevention, treatment, and management. Appropriate genetic testing, diagnosis, and treatment planning of orofacial clefts by a craniofacial cleft lip/cleft palate team can provide comfort to the patient and patient's parents. This can also lead to proper management and give the team the highest chance for a successful treatment outcome.

#### **2.1.4 Classification**

There are about one hundred different combinations of cleft lip and cleft palate. Having a system in place to properly diagnose the clefts and determine a severity assessment helps in the planning of an appropriate treatment method. An ideal system would be easy to understand, easy to locate and to quantify the cleft lesion, easy to document, easily applicable to computerized data analysis, and should be applicable for both clinical applications and research (Rani and Chickmagalur 2011).

Classification of cleft lip and cleft palate deformities has been through multiple changes over the years, each with a different basis for classifying these orofacial clefts, ranging from anatomic and embryologic considerations to the complexity of the deformity. Davis and Ritchie developed one of the first classification systems in 1922, which was used for years, despite its shortcomings. To date, the Kernahan and Stark's classification system and Kernahan's modified "striped Y" diagram (Figure 2.1.4) is one of the most widely used systems worldwide (Rani and Chickmagalur 2011).

Although classifying cleft lip and cleft palate has cycled through systems relating to the morphological and embryological backgrounds, schemes for classifying cleft lip and/or cleft palate are usually anatomically based. These classifications may include complete or incomplete, unilateral or bilateral, a submucous cleft, and/or bifid uvula (Seifeldin 2016).

### **2.1.5. Prevalence**

Cleft lip and/or cleft palate is the most prevalent congenital craniofacial birth defect. The incidence ratio for cleft lip and/or cleft palate has been reported to be approximately 1:700 live births (Cobourne 2004). Additionally, cleft lip and/or cleft palate is the second most common congenital malformation following clubfoot (Miloro et al. 2004). The occurrence of cleft palate is 6.35 per 10,000 live births. The occurrence of cleft lip, with or without cleft palate, is 10.63 per 10,000 live births (Parker et al. 2010). Within this group of patients born with cleft lip and palate, approximately 75% have maxillary alveolar clefts (Bell et al. 1980).

Unilateral cleft lip and palate is more common than bilateral. Cleft lip and palate is more common on the left side than on the right side. When cleft palate is analyzed alone, it is more common in females and most often associated with other developmental anomalies (Seifeldin 2016). However, if analyzing cleft lip, alveolus, and palate, males are more often affected than females (van Hout et al. 2011).

The incidence of these clefts (alveolus, palate, and lip) also varies between different races. Mongolians have an incidence of 0.55-2.5 per 1,000 births. Caucasians have an incidence of 0.69-2.35 per 1,000 births. And finally, Negroids have an incidence of 0.18-0.82 per 1,000 births (van Hout et al. 2011).

## 2.2. Alveolar Cleft

The term *alveolus* is of Latin origin and refers to a small cavity (Coots 2012). The alveolus is a part of the primary palate and is formed by the fusion of the maxillary prominences approximately at the fifth and sixth weeks of intrauterine development. The primary palate gives rise to structures including: nose, lip, prolabium, and the premaxilla; all of which are anterior to the incisive foramen (van Aalst et al. 2008). The incisive foramen has been determined to be the dividing structure differentiating the primary and secondary palates.

The alveolar processes, found in both the maxilla and mandible, are where the tooth sockets are located. These alveolar processes, and the bone that makes them up, are connected to the teeth via periodontal ligaments. In individuals with alveolar clefts, the individual's permanent teeth, which are above the alveolar cleft, are not sustainable if there is not adequate bone stock placed in the alveolar cleft into which they can erupt. The permanent maxillary canine tooth typically erupts into the alveolar cleft space or becomes impacted. The permanent maxillary lateral incisor tooth erupts either adjacent to the alveolar cleft or into the cleft (Coots 2012).

According to Kang, an alveolar cleft is “a tornado-shaped bone defect in the maxillary arch.” Alveolar clefts occur in response to divergence from normal intrauterine development during frontonasal prominence growth, contact, and fusion. Although maxillary alveolar clefts can occur mesial to either the lateral incisor or canine, the most common location is between the lateral incisor and canine (2017). These three dimensional defects are pyramidal in shape (Figure 2.2.1) with the following boundaries: nasal floor superiorly, posterior alveolus (palate) inferiorly, anterior alveolus anteriorly, and medial/lateral cleft margins determining the medial and lateral borders (Craven et al. 2007).

Alveolar clefts cause a disruption in the continuity of the maxillary arch. This can lead to: early feeding difficulties, nutritional issues, developmental delays, speech difficulties, facial asymmetry, hearing loss, discomfort during and/or following surgical procedures, time

commitments, delayed or ectopic eruption patterns, the need for orthodontic care, and possibly psychosocial issues for the child and/or child's parents (Coots 2012).

## **2.3. Managing Alveolar Clefts**

### **2.3.1. History**

Reconstruction of alveolar cleft is believed to be introduced by von Eiselsberg in the early 20<sup>th</sup> century. He used autologous tissue to assist with the reconstruction process. Lexer was the first to describe a nonvascular bone graft. Drachter reported the repair of an alveolar cleft using the tibial bone as a grafting material, while Schmid was the first to utilize this procedure for implanting iliac bone grafts into the defect. Skoog developed a boneless bone graft technique known as gingivoperiosteoplasty (Kang 2017).

Up until the 1970's, "primary bone grafting" was completed while the individual with alveolar cleft was an infant. This was accomplished with rib bone and was the popular surgical procedure used to manage alveolar clefts (Kang 2017). Primary bone grafting involves reconstruction of the alveolar cleft in association with soft tissue repair to the cleft lip. This technique gained popularity because it simultaneously addressed both soft tissue and bony deficit repair. It also was thought this technique would allow for harmonious facial growth and development following the procedure (Seifeldin 2016).

However, there were shortcomings associated with primary alveolar bone grafting. Robertson and Rherm reported adverse developmental effects on maxillary development. Individuals who had primary bone grafting were seen to have midface retrusion and/or anterior cross bites (Dissaux et al. 2016). This led to the currently accepted approach of "secondary bone grafting."

Secondary bone grafting is the most recognized surgical approach for managing alveolar defects in cleft lip/cleft palate individuals. It is believed that the shortcomings associated with

primary bone grafts are not as serious of a concern when the procedure is completed later in development (Kang 2017).

### **2.3.2. Goals**

Every individual born with a cleft lip and/or cleft palate should be assessed and evaluated carefully. The individual's breathing and signs of airway obstruction, ability to feed, nutritional intake, weight gain, growth, syndromic associations that require genetic testing, and craniofacial anomalies need to be evaluated. Additionally, it is important to evaluate the severity and type of defect, the width of the defect, position of alveolar segments and premaxilla, nasal deformity, the need for presurgical orthopedics, type of appliance necessary, and prepare the child and parents for surgical repair of cleft (Bagheri et al. 2011). For this reason, it is vital for individuals with clefts to be managed by a specialized craniofacial and cleft lip/cleft palate team.

There are several primary goals when managing the alveolar cleft. The goals of a successful alveolar graft include: creating a continuous maxillary arch, facilitating eruption of permanent teeth, providing adequate bone support, preserving periodontal health of teeth adjacent to the cleft, permitting orthodontic tooth alignment, allowing placement of osseointegrated implants, and improving alar base symmetry. In addition, it is important to contemplate the effects of surgery and timing of this procedure on continued midface development (Bergland et al. 1986; Amanat and Langdon, 1991; Cohen et al. 1993; Dempf et al. 2002; Oberoi et al. 2009; Francis et al. 2013; Linderup et al. 2016; Seifeldin, 2015; Hammoudeh et al. 2017; Fahradyan et al. 2019).

### **2.3.3. Treatment Timing**

Historically, alveolar bone grafts have been completed at three different time periods relative to teeth development: at the time of deciduous dentition, at the time of mixed dentition, and following mixed dentition. Primary bone grafting is performed in the deciduous stage of



dental development, secondary bone grafting is performed during the mixed dentition, and tertiary bone grafting is performed following the mixed dentition (Fahradyan et al. 2019).

Primary bone grafting has been shown to have poor results causing orofacial teams to abandon the technique. To overcome the skeletal, occlusal, and periodontal problems of the ungrafted cleft, secondary bone grafting has become the technique/surgery of choice. This technique was popularized by Abyholm et al. (1981), but Boyne and Sands (1972) receive a lot of the credit for the scientific and biological basis of the technique. Secondary bone grafting of the alveolar cleft is ideally completed before the eruption of and when two-thirds of the root has developed on the cleft side canine tooth. This typically ranges from 7-12 years of age, but the dental age of the patient is a more accurate way to analyze proper treatment timing compared to chronological age (Amanat and Langdon 1991).

The current standard of deciding on an appropriate treatment time is based on the radiographic analysis of the cleft side canine root development; however, this method is also controversial.

#### **2.3.4. Outcomes and Success Rates**

Defining a “successful” unilateral alveolar graft may have different meanings for different specialists. To an oral surgeon, a successful alveolar graft may mean any stability of the grafting material at the post-graft observation. To an orthodontist, a successful alveolar graft may mean the improved ability for the canine to erupt normally and enhanced ability to align teeth within the continuous osseous ridge. Previous studies address success rates for alveolar cleft grafts as either percent bone fill or percent residual cleft defect following the procedure. These methods are becoming the new standard to avoid the difficult identification process in differentiating natural alveolar bone from graft material on CBCT images.

Herford et al. used computed tomography to compare bone morphogenetic protein-induced repair of the premaxillary cleft with the gold standard anterior iliac crest as a graft

material. This study analyzed 12 total subjects. The average age of patients receiving anterior iliac crest graft was ten and the average age of patients receiving bone morphogenetic protein graft was eight. Their post-graft images were captured at 4-months following the surgery and they concluded an average bone fill of 78.1% and 71.7% for anterior iliac crest and bone morphogenetic protein respectively (Herford et al. 2007).

Another study analyzed the percentage of bone fill 1-year post-graft using anterior iliac crest. There were 21 subjects in this study and the average age at the time of alveolar bone grafting was 10 years 7 months +/- 2 years 8 months. CBCT images were used for measuring the volumetric values of the alveolar cleft. The authors concluded an 84.1% bone fill for unilateral alveolar cleft patients with a range of 61.9% to 96.5% (Oberoi et al. 2009).

Francis et al. used occlusal radiographs to compare recombinant human bone morphogenetic protein-2 with autologous iliac crest bone for repairing alveolar clefts. This study analyzed 55 consecutive patients with an average age of 11.8 years. Their post-graft images were captured at an average of 21 months following surgery. The authors defined a successful alveolar graft as, "those with radiographically evident bony bridging at the cleft site for which no subsequent regrafting procedure was necessary." They used the Bergland and Chelsea scale to evaluate the occlusal radiographs. This study concluded a 94.4% success rate for rhBMP-2 and an 84.2% success rate for anterior iliac crest (Francis et al. 2013).

Dickinson et al. studied older alveolar cleft patients to see if there was reduced morbidity and improved healing when using bone morphogenetic protein-2 as a graft material. The average age at surgery was 16.4 +/- 1.5 years and 15.9 +/-1.9 years for the bone morphogenetic protein-2 and anterior iliac crest groups respectively. Panoramic and computed tomography images were captured pre-graft and 1-year post-graft to determine the results. As far as morbidity, the authors concluded bone morphogenetic protein-2 to be superior to anterior iliac crest in the following areas: donor site pain, length of hospital stay, and overall cost of the procedure. As far as bone healing, this study concluded bone morphogenetic protein-2 to have a larger percentage alveolar

defect fill (95%) compared to anterior iliac crest (63%) at the 1-year post-graft scan (Dickinson et al. 2008).

A paper from 2016 analyzed a different grafting material to be used during secondary alveolar graft procedures. Linderup et al. used mandibular symphyseal bone and CBCT images to analyze the success rates of alveolar cleft grafting procedures at 1-year post-graft. 32 total patients were studied with an average age of 9 years 6 months. The authors concluded an 87% bone fill ratio with a range of 47% to 100% post-graft (Linderup et al. 2016).

Hammoudeh et al. conducted a study using occlusal radiographs to compare alveolar bone graft success rates using human bone morphogenetic protein-2 and iliac crest bone for graft materials. The authors defined a successful graft as one that did not require additional surgeries to repair the defect. Functionally, graft success was evaluated based on the cleft side canine eruption pattern. If this canine was able to erupt naturally on its own, the graft was deemed a functional success. This study concluded success rate of alveolar grafts at 88.4% and 90.0% for iliac crest bone and human bone morphogenetic protein-2 respectively (Hammoudeh et al. 2017).

Finally, in 2011 a systematic review was completed on the results of using bone morphogenetic protein-2 for alveolar graft procedures. The use of this tissue engineered graft material has shown favorable results. This study concludes that the use of bone morphogenetic protein-2 has good results in terms of quantity of bone formation within the cleft, shortens the operation time, eliminates the donor site morbidity issue, shortens the hospital stay, and reduces the overall cost (van Hout et al. 2011).

In addition to overall success rates for secondary alveolar grafts, a number of factors are believed to influence the outcome of alveolar bone grafting. Independent variables have previously been analyzed to determine their effects on these outcomes. According to previous studies, there is no significant difference between unilateral and bilateral cleft patients in terms of success rates. The size of the preoperative alveolar cleft did not appear to influence the success rates. There was also no significant difference in outcomes when comparing if an adjacent lateral

incisor was present or not. The developmental stage of the cleft side canine did not statistically show an effect on the outcomes. And finally, there was no difference in outcomes when comparing gender differences (Linderup et al. 2016; Oberoi et al. 2009).

#### **2.4. Materials Used for Secondary Alveolar Grafts**

Grafting orofacial clefts dates back to the early twentieth century. In 1901, Von Eiselsberg was the first surgeon to use autogenous bone to graft the maxillary cleft by way of a free bone sample of the little finger. Lexer was also on the forefront of these methods in 1908. In 1914, Drachter was the first to report the successful closure of a cleft with tibial bone and periosteum (Lilja 2009). Since these first methods were introduced, various graft materials, including tibia, calvarium, mandible, rib, and anterior iliac crest have been analyzed and compared (Linderup et al. 2016). The hope is to find an alveolar cleft graft material that will allow for the elimination of donor site morbidity, prolonged hospital stays, increased surgical cost, and post-graft pain while delivering high success rates and allowing for proper physiological and psychological function of the maxillofacial complex.

Cortical and cancellous bones can be used for grafting orofacial clefts, but cancellous bone seems better due to the cell transfer and revascularization noticed in osteoinduction and osteoconduction. Fresh autologous cancellous bone has been reported to be the most ideal bone graft source because of the increased amount of osteogenic precursor cells within the matrix (Kang 2017; Seifeldin 2016). Cortical bone takes longer to incorporate at the graft site because it relies on vascular ingrowth in a process called “creeping substitution.” In addition to being better in osteoinduction and osteoconduction processes, cancellous bone has also been shown to allow tooth eruption more often (Coots 2012). Numerous autologous bone donor sites have been used and studied in hopes to determine an appropriate graft material to meet the goals listed previously.

Bosker and van Dijk were the first to report the use of mandibular symphysis bone as a grafting material for secondary alveolar grafts in 1980. The mandible has the same embryonic origin as the maxilla and because it is an intramembranous bone, revascularization is fast and resorption is minimal (Kang 2017; Seifeldin 2016). This material seemed attractive because it displayed low morbidity while allowing for satisfactory success rates. Some of the advantages include: restriction to one intraoral operation site, shorter time in the hospital, minimal discomfort, and an incision located in the lower labial sulcus leading to an invisible scar. Disadvantages associated with mandibular symphysis include: limited volume of bone available for grafting bilateral clefts, a small operation site eliminates the possibility of two operative teams working at the same time, increased amount of cortical bone in the donor material, and possible injury to the mental nerve that could result in changes in sensitivity of adjacent teeth/soft tissues (Coots 2012; Linderup et al. 2016; Rawashdeh and Telfah 2008).

As stated previously, Drachter was the first to use tibial bone to reconstruct alveolar clefts in 1914. Since then, few authors have reported the tibia as a donor site for alveolar grafts. The tibia has been extensively used in orthopedic surgeries and is a popular material among maxillofacial surgeons, however most of the procedures completed with tibia material is seen in adult patients, and mainly for trauma incidences. Some of the advantages of using tibia as a graft material include: shorter operation time, minimal scarring, shorter hospital stay, and quicker ambulation. On the contrary, the disadvantages of using the tibia as a graft material seem to far outweigh the advantages. These include: lack of available material in younger patients, close proximity to the growing epiphyseal cartilage, possibly needing to take material from both legs, proximal tibial fractures (reported in the range of 0-2.7%), and the need to avoid contact sports for at least three months (Kang 2017; Rawashdeh and Telfah 2008; Seifeldin 2016).

Another graft material that has been studied is calvarial bone. This material has shown similar success rates for alveolar grafts when compared to iliac crest bone. Some of the

advantages for using calvarial bone include: inconspicuous scar formation, lack of functional deformity, appropriate surgical field, and volume of bone that can be harvested. However, there are high risk disadvantages that go along with this material and complication rates range from 0.25-5.5%. These include: long operative time, wound infection, minimal cancellous bone, thin bone, and intracranial complications such as hematoma, dural tear, dural exposure, and cerebrospinal fluid leakage. Calvarial bone is most often suggested for patients who do not have a high chance of multiple head injuries such as athletes (Kang 2017; Rawashdeh and Telfah 2008; Seifeldin 2016).

Autogenous bone taken from the anterior iliac crest is considered the most common method and optimal material for grafting alveolar clefts and is thus termed the “gold standard bone graft.” It has also been shown that this material should be the standardized graft to which other types of alveolar bone grafts should be compared. Some advantages of using anterior iliac crest include: provides a large quantity of cancellous bone, has easy surgical access, great osteogenic potential with abundant pluripotent osteogenic precursor cells. The disadvantages associated with using iliac crest for grafting alveolar clefts include: hematoma, pain, delayed ambulation, prolonged hospital stay, possible scarring, and risk of cutaneous nerve injury (Kang 2017; Rawashdeh and Telfah 2008; Seifeldin 2016). To help reduce these complications, limited incision, reduced musculature elevation, hemostasis, adequate pain control, and quick ambulation are suggested (Kang 2017).

To eliminate the donor site morbidity and other complication with autogenous bone grafts, tissue engineering has become a popular concept for developing an alternative to the previously studied graft materials used for secondary alveolar grafting procedures. Three vital components are necessary for tissue engineering and include: bone-forming cells, osteoinductive growth hormone, and an osteoconductive scaffold. The scaffold provides mechanical support, mimics the bony matrix, and guides the formation of bone in the defect area. This scaffold can serve as a carrier for the osteoinductive growth hormone. This hormone is thus delivered locally

and ideally over a sustained period of time to recruit mesenchymal stem cells to differentiate into osteogenic cells (van Hout et al. 2011).

With these novel methods of producing and delivering graft material alternatives, many of these materials have been studied and their success rates have been analyzed. One of the most commonly used substitutes for secondary alveolar grafts is recombinant human bone morphogenetic protein-2 (rhBMP-2). rhBMP-2 was initially identified by Marshall Urist, an orthopedic surgeon conducting research on bone mineralization, and Strates in the 1960's. These proteins are involved in the natural formation and development of the human skeleton. Very small quantities are contained in the mature skeleton and are associated with bone maintenance and fracture repair. Early on, Urist placed demineralized, lyophilized segments of allogeneic bone matrix into muscle pockets in rabbits and watched as bone was formed. This led him to postulate the concept that these proteins, located within the matrix, can promote the formation of osteoblasts (Chin et al. 2005).

rhBMP-2 belongs to the transforming growth factor- $\beta$  superfamily of proteins. This protein induces bone and cartilage formation through signal pathways (Hammoudeh et al. 2017). They are essential for skeletogenesis in the embryo and for bone remodeling throughout life. Supraphysiologic levels of these proteins promote de novo bone generation (Francis et al. 2013).

Bone morphogenetic proteins (BMPs) in general were approved by the United States Food and Drug Administration (FDA) for maxillary sinus augmentation in 2004 and alveolar ridge augmentation following dental extraction in 2007. Although rhBMP-2 has been shown to have favorable outcomes as an alternative grafting material, it has been considered to be off-label for the use of grafting alveolar clefts (Francis et al. 2013; van Hout et al. 2011). Despite the approval for augmentation procedures, rhBMP-2 has raised concerns over its use for grafting orofacial clefts. An initial U.S Food and Drug Administration warning was issued after accounts of post-graft dysphagia and airway compromise due to swelling in patients who received it around the cervical spine. Another U.S FDA warning was issued in 2015 for safety issues arising

with the use of rhBMP-2 in the pediatric population out of concern for insufficient data to represent long-term safety and efficacy (Hammoudeh et al. 2017). However, in recent years several groups and research teams have reported experiences using rhBMP-2 off-label for alveolar cleft reconstruction in the pediatric population (Francis et al. 2013).

A study conducted at the Children's Hospital Los Angeles prior to the U.S. FDA warning on rhBMP-2 compared the outcomes of using rhBMP-2 vs iliac crest as a grafting material for alveolar clefts in the pediatric population. A demineralized bone matrix was used as the carrying scaffold during the procedures. During a 10-year period, this study did not observe an increase in evidence of infection, heterotopic ossification, malignant transformation, or airway compromise for the patients receiving rhBMP-2 (Hammoudeh et al. 2017). This study was a pivotal point in the introduction of rhBMP-2 as an attractive alternative to the previous gold standard, iliac crest, for secondary grafting of alveolar clefts in younger patients. rhBMP-2 has also been shown to display improved bone healing and decreased post-graft pain in adult patients receiving alveolar cleft grafts when compared to iliac crest (Dickinson et al. 2008).

Overall, rhBMP-2 appears to be an attractive alternative graft material to the previous gold standard, iliac crest. It would allow for the elimination of donor site morbidity, decrease the post-graft pain, reduce the overall cost of the procedure, limit hospital stay, and promote post-graft ambulation while still allowing for high success rates for alveolar graft procedures.

## **2.5. Cone Beam Computed Tomography to Evaluate Alveolar Graft Procedures**

Up until recently, the majority of secondary alveolar graft studies have been conducted using two-dimensional radiographs, such as occlusal, panoramic, and periapical films. These studies have used these images, along with either the Bergland scale (Figure 2.5.1) or Chelsea scale (Figure 2.5.2), to evaluate the alveolar cleft defect area and to understand the outcomes of secondary alveolar grafts (Trindade et al. 2005). In the Bergland scale system, a four-point system was used to classify each graft depending on the coronal level of the interdental bone



compared to normal levels. One of the main shortcomings with this system was that the graft was compared only at the interdental level using normal bone levels for reference values (Seifeldin 2016).

There are obvious shortcomings in attempting to determine the outcomes of alveolar bone grafts from 2-dimensional images. They do not accurately quantify the 3-dimensional pyramidal shape of the alveolar cleft of interest and could initiate errors when determining the true defect volume. Computed tomography (CT) was one of the first radiographic techniques used to 3-dimensionally view the alveolar cleft entirely. Because traditional CT images had high radiation doses, long scan times, and low quality/low resolution images, other radiographic methods were discovered. Between 1998 and 1999, cone-beam (CB) systems were introduced for oral and maxillofacial images and replaced the traditional CT images allowing for limited radiation doses (approximately 15-times less), minimal scanning time (10-70 seconds), and high quality/resolution images (Seifeldin 2016). Over the last decade, the orthodontic and dental field, as a whole, has adopted the use of CBCT for diagnosis, treatment planning, and reduction of radiation dose compared to conventional tomography (Ludlow et al. 2015).

Various 3-dimensional software have been reported and used in the identification, segmentation, and quantification of orofacial and alveolar clefts. Software such as Amira 3.1.1, Mimics 15.0; Materialise Interactive Medical Image Control System, and ITK-SNAP 3.8.0 have been reported throughout the orthodontic literature in regards to determining/measuring volumetric values of alveolar clefts.

## CHAPTER 3: RESEARCH HYPOTHESIS & SPECIFIC AIMS

### 3.1. Statement of the Problem

Bone grafting of alveolar clefts is an essential component in the contemporary management of patients with orofacial clefts. The search for an appropriate alternative to the autogenous graft material, such as anterior iliac crest, has included experiments with many substitutes. However, alveolar bone graft outcomes of rhBMP-2, as an alternative to autogenous sources, in unilateral alveolar cleft patients is yet to be studied. Determining the appropriate timing for this procedure to produce the best outcome is also still controversial. Chronological age, root development of the cleft side canine, and stage of dental maturity have all been used to estimate the most appropriate time to graft the alveolar cleft. Additionally, there may be other factors that need to be analyzed to determine the proper timing of alveolar bone graft procedures and to better estimate the success rates of these grafts.

Intraoral occlusal and periapical radiographs have been used to evaluate bone fill within an alveolar cleft and to map segmentally the height, thickness, and position of bone adjacent to the roots of the cleft. With the shortcomings associated with analyzing a three dimensional structure using two dimensional radiographs, the use of three-dimensional CBCT radiography has become a popular alternative. CBCT imaging would allow one to better appreciate the severity, location, and overall graft outcome of unilateral alveolar clefts. Since this technology is readily available and reliable, it could be utilized to investigate the clefts pre-graft as well as post-graft to determine the overall success rates. This knowledge is essential to be able to foresee what variables affect the graft outcomes. This information can be used to aid practitioners in understanding the severity of the orofacial cleft, treatment planning the alveolar graft procedure, and assist in preventing negative sequelae.

### **3.2. Central Research Hypothesis**

The central research hypothesis is that there will be a difference in secondary alveolar graft success rates when comparing: gender, age, side of the cleft, canine root development, canine angulation in both the coronal and sagittal planes, and canine distance from the occlusal plane and their effects on these outcomes using 3-dimensional software for analysis.

### **3.3. Specific Aims**

1) To determine the overall success rate of using rhBMP-2 for unilateral secondary alveolar cleft grafts using CBCT radiography.

2) To determine if gender, age, side of the cleft, canine root development, canine angulation in both the coronal and sagittal planes, or canine distance from the occlusal plane have an influence on these success rates using CBCT radiography.

## CHAPTER 4: MATERIALS & METHODS

### 4.1. Study Design

This study is a retrospective comparison of pretreatment and post-treatment CBCT images of patients with unilateral alveolar clefts who received secondary alveolar bone grafts at the University of Nebraska Medical Center Oral and Maxillofacial Surgery Center in Omaha, Nebraska. This study protocol was reviewed and approved by the University of Nebraska Medical Center Institutional Review Board (#113-20-EP) and the Boys Town National Research Hospital Institutional Review Board (#20-03-X).

#### 4.1.1. Data Collection

It is routine for patients with cleft lip and palate to see a craniofacial and cleft lip/cleft palate team for proper management. The team at Boys Town National Research Hospital consists of a wide range of specialists including: pediatrician, orthodontist, oral surgeon, plastic surgeon, otolaryngologist, speech pathologist, audiologist, craniofacial nurse, genetic counselor, social worker, and a nutritionist. Dr. V.D. is the oral surgeon on this Boys Town National Research Hospital team. He routinely collects a pre-graft CBCT radiograph for the orofacial cleft patients requiring alveolar cleft grafting procedures. The information from this image is used to diagnose problems, create treatment objectives, and formulate a comprehensive treatment plan. Additionally, Dr. V.D. routinely captures a 6-month post-graft CBCT radiograph to monitor the success rates and analyze the graft material uptake/residual defect.

Consecutive patients with unilateral alveolar clefts who received secondary alveolar bone grafts from Dr. V.D., from June 1, 2014 to January 1, 2020, were selected for this study. Inclusion criteria for this study included: patient age between 7-13 years old at the time of the alveolar graft surgery, patients with unilateral alveolar cleft, patients who used rhBMP-2 as the graft material, and access to available pre-graft and post-graft CBCT images. Exclusion criteria

included patients who received an alveolar bone graft previously, patients who have had a failed bone graft, those with bilateral alveolar clefts, and patients who received anterior iliac crest bone graft. 24 patients were included in this study and their pre-graft and post-graft CBCT images were analyzed.

CBCT images were acquired using a Kodak 9500 3D scanner (Kodak Dental Systems, Carestream Health, Rochester, NY). The orofacial cleft was captured with the following settings: tube potential of 90kV, current of 10mA, 3.6 second exposure time, 0.2mm scanning layer thickness, and 200um voxel size. All data sets with DICOM (Digital Imaging and Communications in Medicine) format were transferred to Invivo5 (version 5.2; Anatomage Dental, San Jose, California) for storage and interpretation.

The DICOM data were exported and scanned to university protected disks at the University of Nebraska Medical Center Oral and Maxillofacial Surgery Center. All data was uploaded to the University of Nebraska Medical Center protected database to ensure patient confidentiality. DICOM data were imported to Precision Workstation T3600 desktop computer (Dell, Round Rock, TX) with appropriate imaging software as described in subsequent sections. All images were viewed on a 60.47 cm LED widescreen display monitor screen (Dell) having a resolution of 1920 x 1080 pixels.

Demographic and treatment variables were recorded for each patient based on the information obtained from the patients' charts. Age of the patient at the time of surgery, graft material used during the procedure, side of the unilateral cleft, and gender of the patient were documented for analysis.

#### **4.1.2. Surgical Technique**

All grafting procedures were performed under general anesthesia with orotracheal intubation. Patients received preoperative prophylactic antibiotic therapy of cefazolin or clindamycin, if allergic to cefazolin. A one surgeon team completed the unilateral grafts using

rhBMP-2 (INFUSE, Medtronic; Memphis, Tennessee). The same surgeon, Dr. V.D., performed all the procedures to help standardize the case results. Deciduous and supernumerary teeth in the direct vicinity of the unilateral alveolar cleft were extracted one to three months prior to the surgery. This was completed to aid in grafting outcomes and facilitate mucosal flap design utilizing increased keratinized epithelium.

The surgical procedure for grafting of unilateral alveolar clefts was followed as described by Boyne and Sands (Boyne and Sands 1972) with and without the modification of strut technique described by Stoelting et al. (Stoelting et al. 1990). Several other modifications were used during these surgical procedures including: the use of 4-0 Vicryl to close the nasal mucosa, the use of 3-0 and 4-0 Vicryl to close the oral mucosal flaps, and the application of cyanoacrylate to the reconstructed nasal floor and oral mucosal tissues after closure.

For grafting these unilateral alveolar cleft patients, 0.7cc to 1.4cc (1.05mg to 2.10mg) rhBMP-2 with acellular collagen sponge carrier was used. An allogeneic demineralized human cortical bone strut (OsteoWrap, Bacterin; Belgrade, Montana) was also used during the procedure.

Postoperatively, all patients were treated with five days of cephalexin or clindamycin, advised to have a soft diet for one month, and no strenuous activity recommended for two weeks.

#### **4.2. Linear Measurements**

Root lengths of the maxillary canines were measured in millimeters to the nearest hundredth decimal value with specific attention given to the canine on the side of the alveolar cleft. These lengths were measured on CBCT images within the open source segmentation ITK-SNAP 3.8.0 software. Measurements were taken at the following time points: pre-graft and 6-month post-graft. Two separate linear measurements were taken from the cemento-enamel junction (CEJ) to the apex of the tooth in the CBCT layer/slice representing the direct long axis of the canine tooth (Figure 4.2.1). The method for measuring root length was based on methods in

previous studies. The canine root lengths were compared to average mature maxillary canine root length values reported to determine the percentage of canine root development at the time of alveolar grafting. The average mature maxillary canine root lengths used as references were 15.83 +/- 1.49mm and 15.23 +/- 1.78mm for males and females respectively (Kim et al. 2013).

CBCT images were analyzed using ITK-SNAP 3.8.0 in both the coronal and sagittal sections to determine the angulation of the cleft side maxillary canine tooth in relation to a true perpendicular reference line. These values were measured in degrees and recorded to the nearest tenth decimal value. In the coronal section, a reference line was traced on the true vertical crosshair. Then, a second line was traced through the long axis of the cleft side canine passing through the apex of the tooth (Figure 4.2.2). These angular measurements were recorded for both the pre-graft and post-graft time periods with attention given to the pre-graft values.

Additionally, the angulation of the cleft side maxillary canine tooth was measured in the sagittal section. In this view, a reference line was traced on the true horizontal crosshair. A second line was traced through the long axis of the cleft side canine passing through the apex of the tooth (Figure 4.2.3). These values were recorded for both the pre-graft and post-graft time periods with attention given to the pre-graft values.

The final linear measurement measured was the distance of the cleft side canine tooth to the defined occlusal plane. This was measured in millimeters to the nearest hundredth decimal. Using the ITK-SNAP 3.8.0 software, the CBCT images were viewed in the sagittal section. A reference line was created from the most inferior aspect of the mesial cusps on the permanent first molar to the most inferior portion of the central incisor on the alveolar cleft side (through all layers/slices). This reference line was defined as the occlusal plane in this study for all patients. Next, a line was inserted from the most inferior tip of the cleft side canine tooth to the defined occlusal plane reference line. These two lines always formed a 90-degree angle at their intersection. These values were recorded for both the pre-graft and post-graft time periods with attention given to the pre-graft values.

Two investigators (L.P. and S.P.) each independently completed the root length measurements on 10 patients (20 CBCT scans). After a minimum of 2 weeks, these same 10 patients (20 CBCT scans) were analyzed by the same two investigators independently. These measurements were used to determine the intra-examiner and inter-examiner reliability of the method used. Once the reliability of the method was established, each investigator completed the root length measurements for one-half of the total sample number.

The cleft side canine angulation measurements and distance from the occlusal plane measurement were performed by investigator L.P. Again, these three measurements were initially completed on 10 patients (20 CBCT scans). After a minimum of 2 weeks, these same 10 patients (20 CBCT scans) were analyzed by the same investigator. These measurements were used to determine the intra-examiner reliability of the method.

#### **4.3. Volumetric Measurements**

The unilateral maxillary alveolar cleft volumes were determined from the pre-graft and 6-month post-graft CBCT images using the open source segmentation software ITK-SNAP 3.8.0. These volumes were measured in cubic millimeters to the nearest hundredth decimal.

The first step in segmentation was using the semi-automatic, or “active contour segmentation mode (5)”, feature in ITK-SNAP 3.8.0. A large region of interest was set in the axial, coronal, and sagittal planes to encompass the desired alveolar cleft defect as well as a large portion of the maxillary arch and adjacent teeth (Figure 4.3.1). The “Active Label” was changed to a green color, representing bone and/or hard tissue. The pre-segmentation mode was used to adjust the contrast and instruct the software algorithm to separate bone/teeth voxels from soft tissue voxels. Within the inverted image, the upper threshold limit was increased to the maximum to limit variability between pretreatment and post-treatment images. The lower threshold limit was chosen by the investigator, for each CBCT image, based on adequate bone to soft tissue differentiation. The smoothness parameter was also set to the maximum value to help standardize



the results and limit inaccurate segmentation (Figure 4.3.2). The initialization mode allowed the investigator to place pre-set bubbles to communicate areas of interest to the software (Figure 4.3.3). Other parameters used during the auto-segmentation feature were setting the step size to 2 and allowing the iteration to run until 600 and 1000 for pre-graft and post-graft CBCT images respectively. Automatic segmentation was allowed to proceed until the raw segmentation began to involve adjacent structures (Figure 4.3.4).

Once the bone and/or hard tissues were segmented out, the polygon mode (3) was used for manual segmentation of the alveolar cleft defect. The feature allows for segmentation in the three orthogonal slices. The “Active Label” was changed to a red color, representing soft tissue, and the segmentation could be painted in any “clear labels” within the ITK-SNAP software (Figure 4.3.5). The polygon mode tool was used to trace out the defect through all slices included in the region of interest that was set based on previous papers. The protocol for setting up the region of interest was adopted from and very similar to that of Linderup (Linderup et al. 2015). The boundaries for the region of interest can be seen in Table 4.3.1. The superior boundary was determined to be ten slices inferior to the anterior nasal spine (ANS); confirmed on the coronal section as a radiopaque dot. The inferior boundary was determined to be the most apical portion of the palatal CEJ of the adjacent tooth. The anterior and posterior boundaries were determined by the anatomical structure of the contralateral alveolar ridge within the slice being analyzed. The medial and lateral boundaries were determined by the initial auto-segmentation process of labeling the bone and/or hard tissues.

Two investigators performed the volumetric measurements of the unilateral alveolar cleft defects. Both investigators were calibrated to eliminate any bias or structural identification errors during manual segmentation. These calibrations were used to minimize the human error presented in the potential artistic interpretation. After the final segmentation was achieved for the region of interest (Figure 4.3.6), the volumetric value was recorded from the “volumes and statistics” tab in ITK-SNAP 3.8.0. (Figure 4.3.7).

Two investigators (L.P. and S.P.) each independently completed the unilateral alveolar cleft volume measurements on 10 patients (20 CBCT scans). After a minimum of 2 weeks, these same 10 patients (20 CBCT scans) were analyzed by the same two researchers independently. These measurements were used to determine the intra-examiner and inter-examiner reliability of the method used. Once the reliability of the method was established, each researcher completed the volumetric measurements for one-half of the total sample number.

#### **4.4. Statistical Analysis**

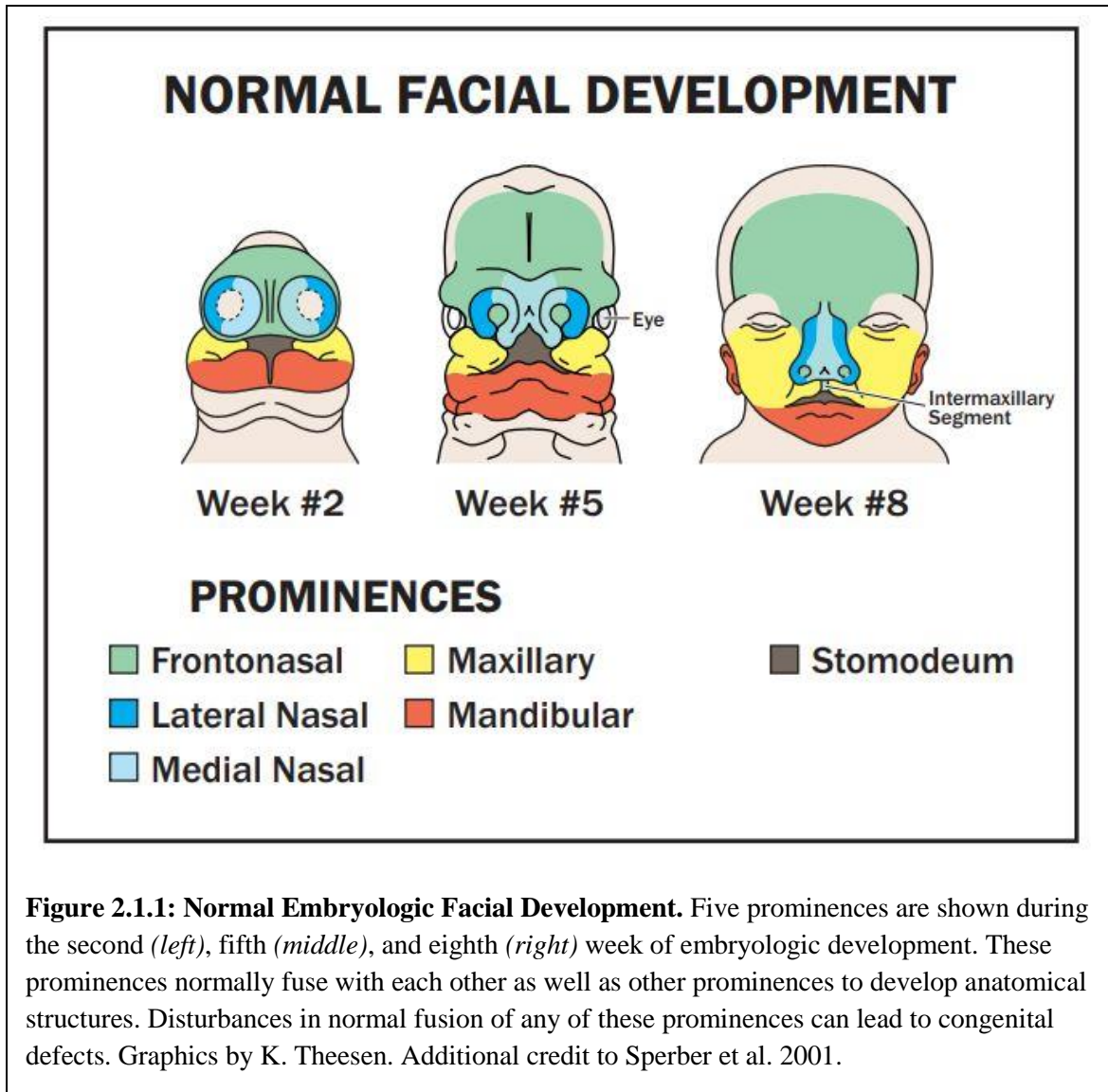
All data were entered into Excel (version 2016; Microsoft, Redmond, Wash). The PROC GLIMMIX procedure in SAS 9.4 (SAS Institute; Cary, NC) was used to analyze the percent residual defect in relation to the explanatory variables of interest. Residual and quantile-quantile plots (QQ-plots) were used to assess model fit. A generalized linear model following a beta distribution with a logit link was used to account for the underlying distribution of the percent residual defect. When differences occurred, least significant difference (LSD) was reported at the  $\alpha = 0.05$  level. A total sample size of 24 subjects was analyzed for the volumetric and linear measurements.

To assess the reliability of the methods used in this study, duplicate measurements were taken on ten consecutive patients at least two weeks apart. Intra-class correlation coefficients (ICCs) were calculated for intra-examiner and inter-examiner reliability using R version 3.6.3 (R Core Team; Vienna, Austria). ICC3 values were used when all subjects are rated by the same raters who are assumed to be the entire population of raters. These values are reported because we are interested in how investigators (LP and SP) are rating the measurements and do not care to extend it to other potential raters.

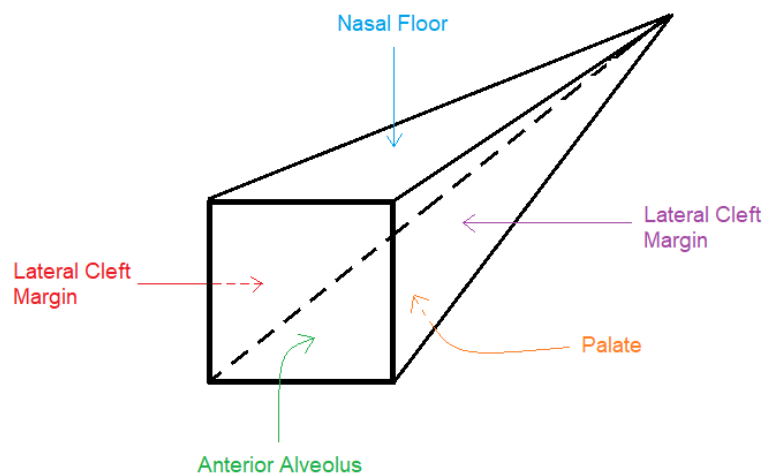
#### **4.5. Intra-examiner and Inter-examiner Reliability**

Intra-examiner reliability was measured with intra-class correlation coefficients (ICCs) using R version 3.6.3 (R Core Team; Vienna, Austria). It was determined by repeating the volumetric and cleft side canine root length linear measurements on ten patients by the original investigator (LP or SP) at least two weeks after the initial measurements on pre-graft and post-graft CBCT images. Intra-examiner reliability was also measured for the cleft side canine angulation and distance from the occlusal plane linear measurements. These were measured by investigator (LP) on ten patients. At least two weeks later, these measurements were repeated on the same ten patients by the same investigator (LP) for the pre-graft and post-graft CBCT images.

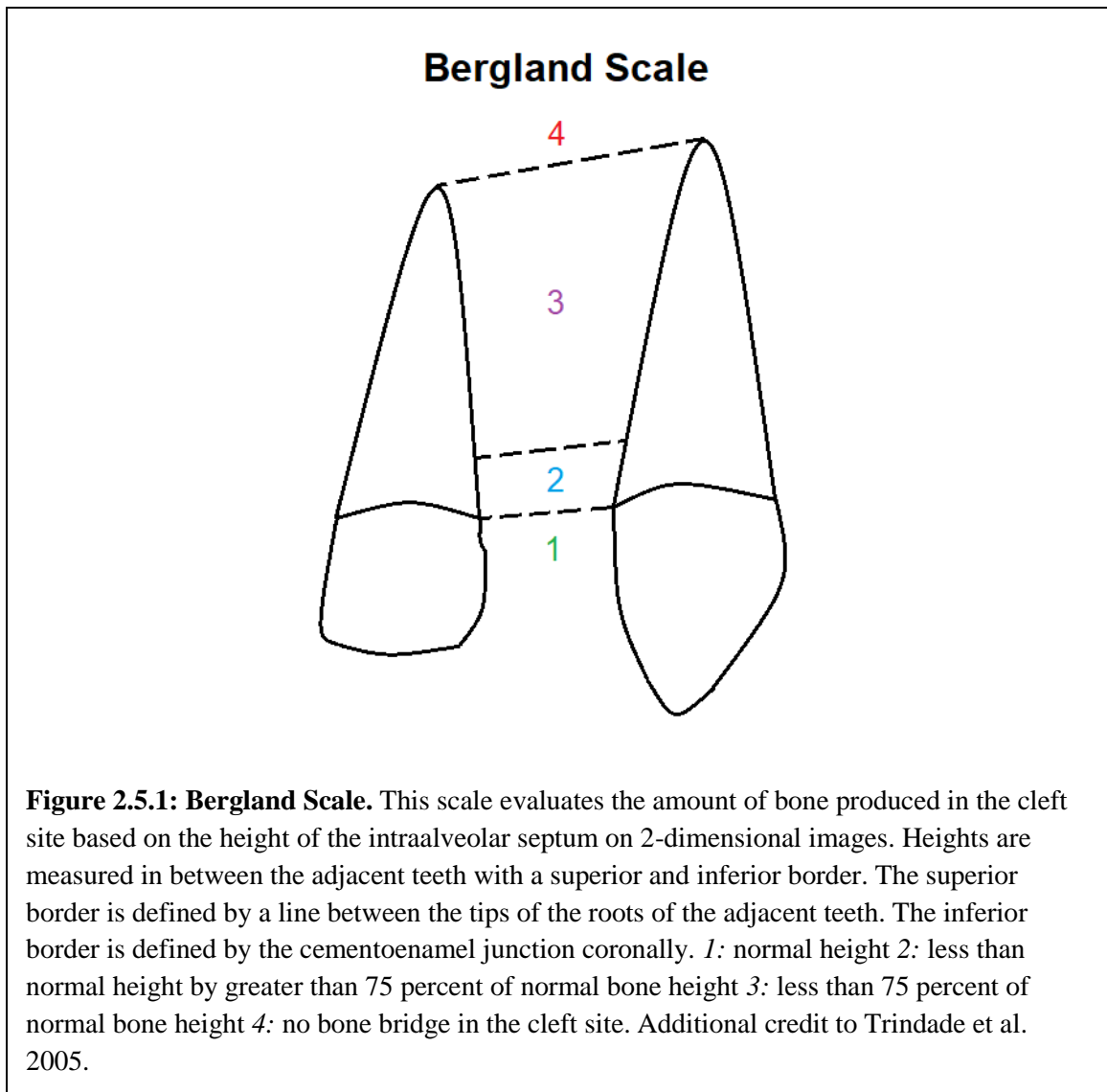
Inter-examiner reliability was determined by comparing the volumetric and cleft side canine root length linear measurements on ten patients for pre-graft and post-graft CBCT images using R version 3.6.3 (R Core Team; Vienna, Austria). The inter-examiner reliability was determined on the same ten patients selected for the intra-examiner reliability test. Again, the inter-examiner reliability was measured with intra-class correlation coefficients (ICC3).

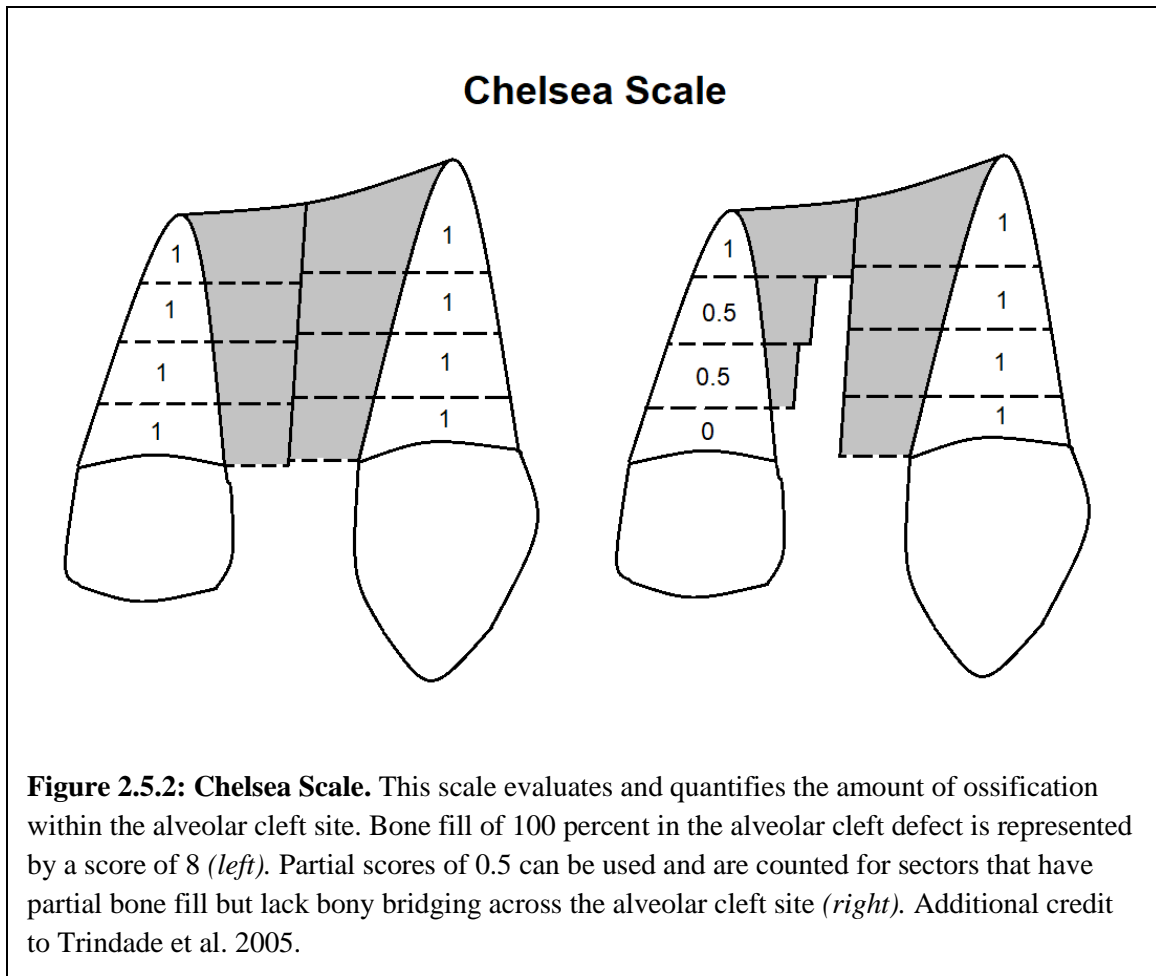






**Figure 2.2.1: Alveolar Cleft Shape.** Classic pyramidal shape of an alveolar cleft. The medial and lateral boundaries are determined by the extent of the cleft (red and purple text above). The superior boundary is determined by the nasal floor (blue text) and the inferior boundary is determined by the palate/posterior alveolus (orange text). The anterior boundary is determined by the anterior portion of the alveolus (green text). Additional credit to Craven et al. 2007.

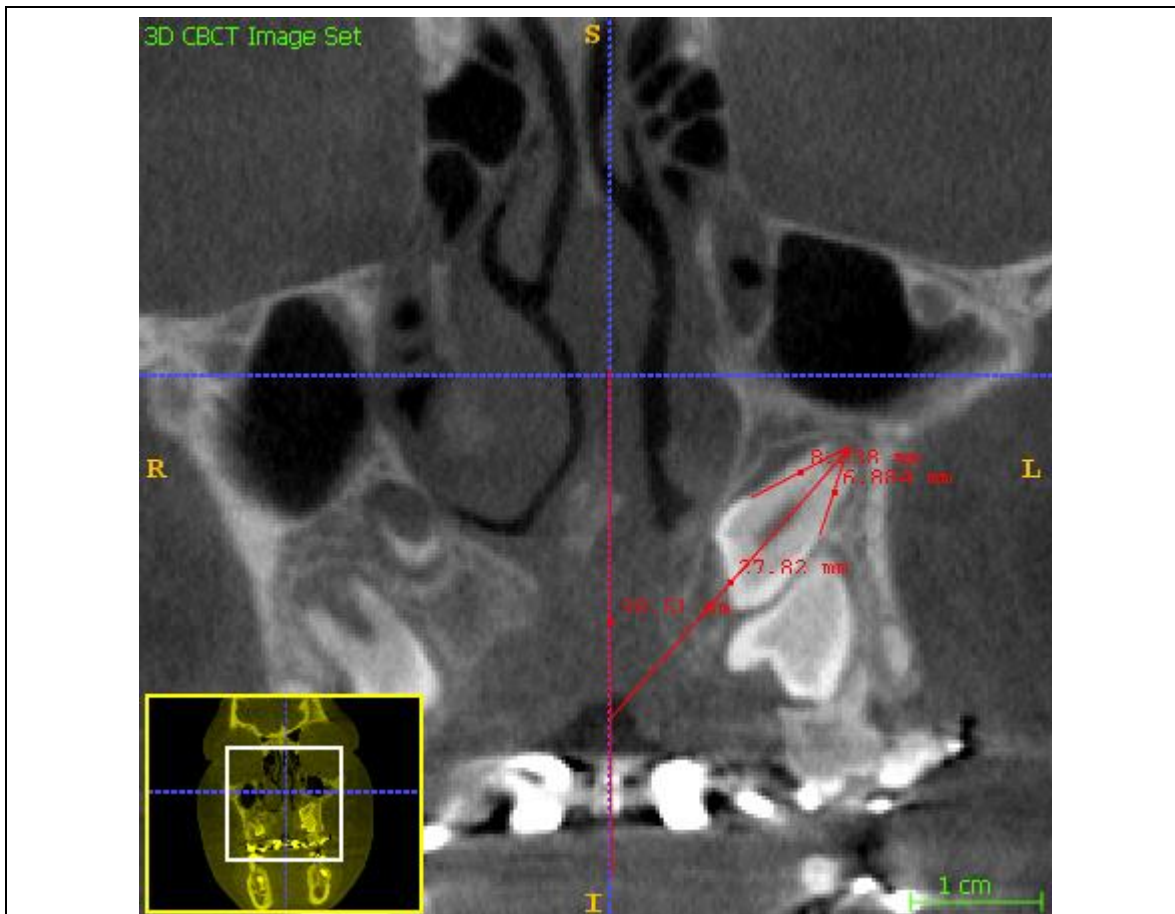








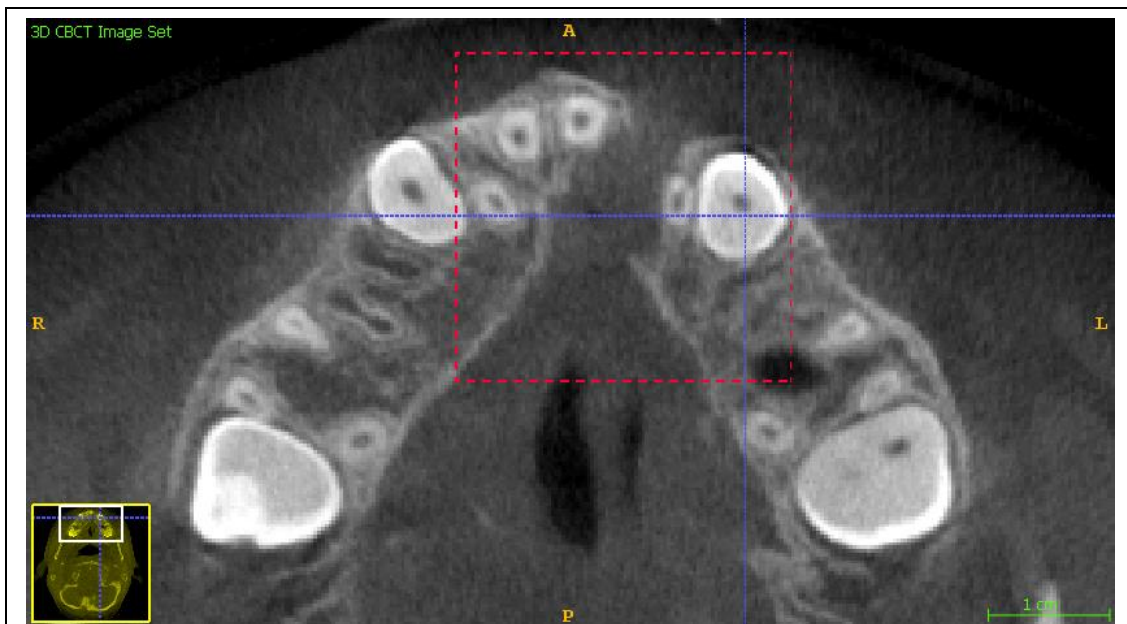
**Figure 4.2.1: Cleft Side Canine Root Length Measurement.** Sagittal view of an immature canine on the side of the unilateral alveolar cleft. Two separate linear measurements were taken from the cemento-enamel junction (CEJ) to the level of the apex in the CBCT layer/slice most accurately representing the direct long axis of the canine tooth. This was usually determined in the coronal or sagittal (shown above) views within the ITK-SNAP 3.8.0 software. The two values were averaged and the mean value was recorded for comparison to previously reported adult canine root length measurements.



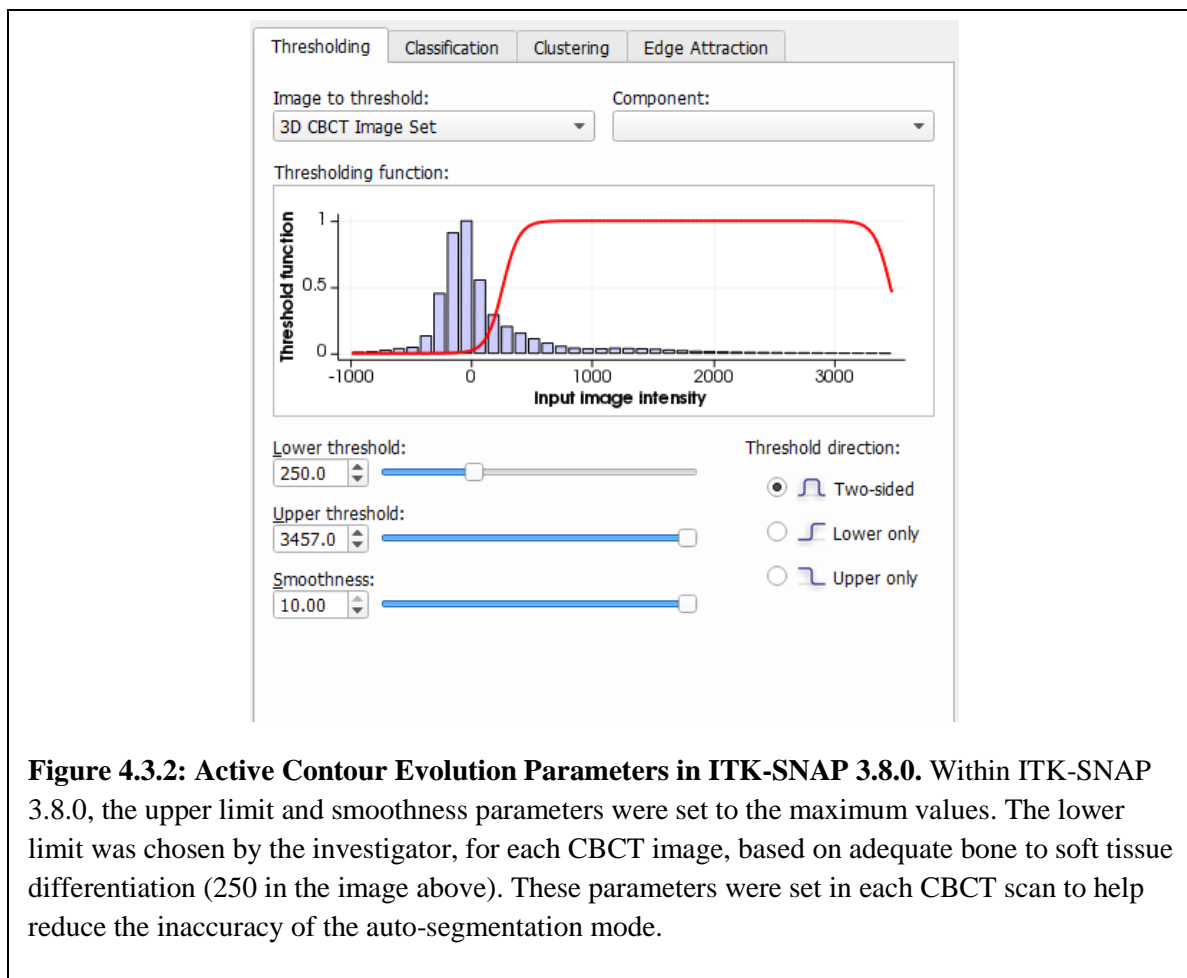
**Figure 4.2.2: Cleft Side Canine Angulation; Coronal Section.** Coronal view of the cleft side canine within ITK-SNAP 3.8.0. The first line (red) was made on the true vertical crosshair approximately located at the midline. The second line (also red) was traced down the long axis of the cleft side canine tooth. The software automatically calculated the angle formed between these two lines and this value was recorded.

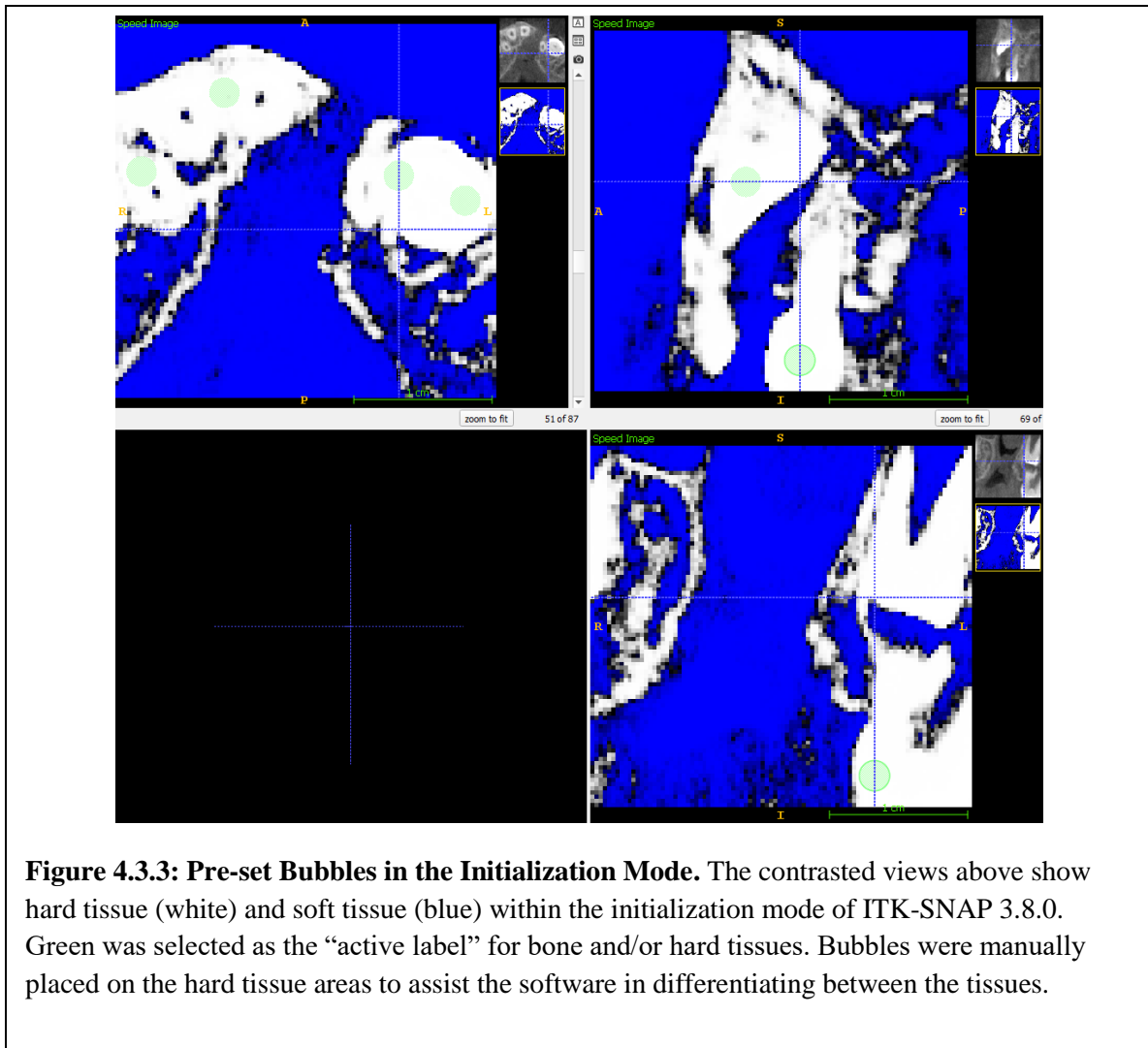


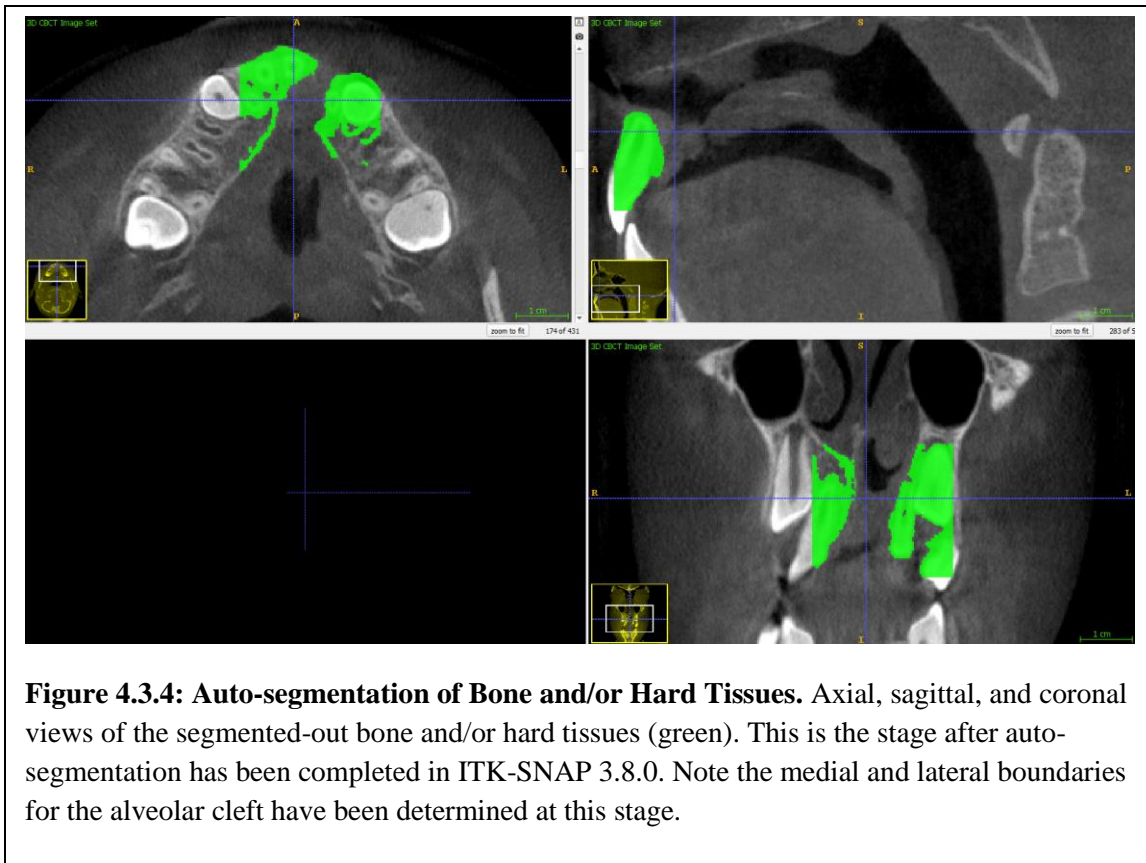
**Figure 4.2.3: Cleft Side Canine Angulation; Sagittal Section.** Sagittal view of the cleft side canine within ITK-SNAP 3.8.0. The first line (red) was made on the true horizontal crosshair. The second line (also red) was traced down the long axis of the cleft side canine tooth. The software automatically calculated the angle formed between these two lines and this value was recorded.



**Figure 4.3.1: Region of Interest for Semi-automatic Mode.** Axial view of the region of interest for the semi-automatic mode within ITK-SNAP 3.8.0. It has been set in the axial, sagittal, and coronal planes. This region (red dotted lines above) includes the unilateral alveolar cleft as well as a large portion of the adjacent maxillary alveolar ridges and teeth.









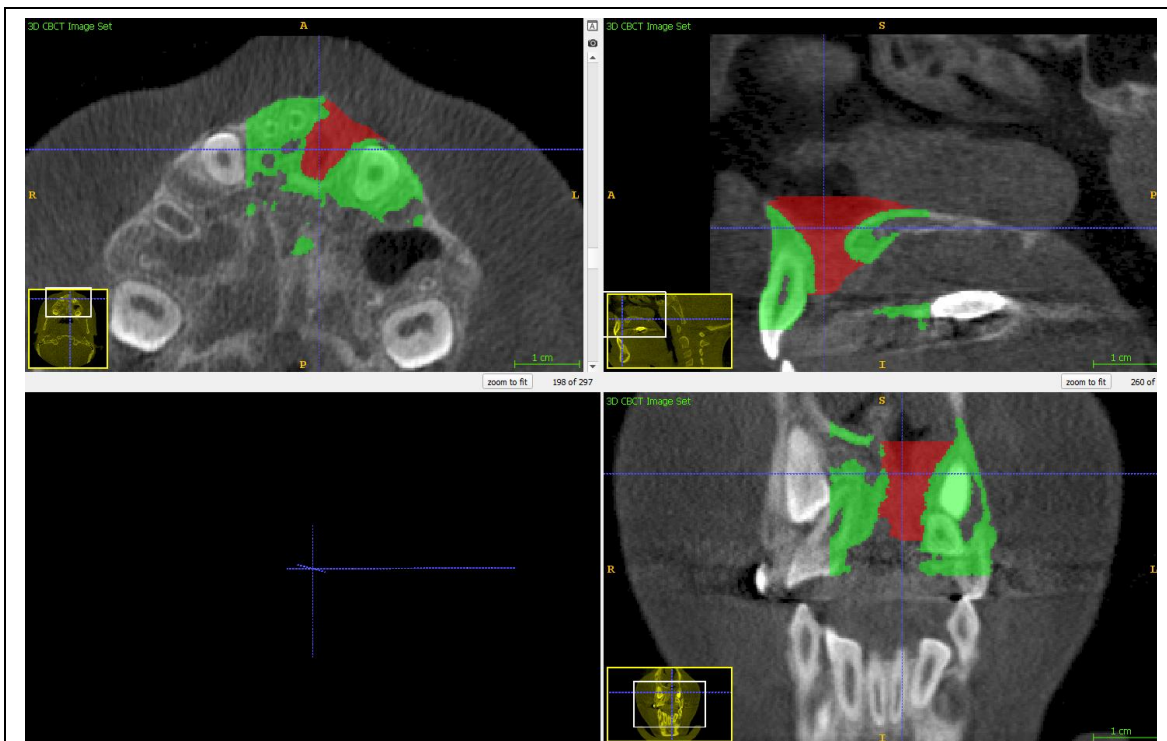


**Figure 4.3.5: Polygon Mode; Manual Segmentation of the Cleft.** Within ITK-SNAP 3.8.0., the unilateral alveolar cleft was manually segmented on the axial view. The superior most boundary was determined by ten slices inferior to ANS and the inferior most boundary was determined by the palatal portion of the CEJ on the adjacent incisor tooth. Through these slices, the anterior and posterior boundaries of the cleft were determined from the anatomical structures of the contralateral side. The software filled in the defect in all three planes shown above (red color).



### Region of Interest Boundaries

Boundary	Definition
Anterior/Posterior	Mimic the anatomical structures of the contralateral alveolar ridge/bony structures
Medial/Lateral	Determined by the initial auto-segmentation process of labeling the bone and/or hard tissue
Superior	10 slices inferior to the anterior nasal spine (ANS) - this was confirmed on the coronal section as a radiopaque dot
Inferior	Most apical portion of the palatal CEJ of the adjacent tooth (incisor)

**Table 4.3.1: Region of Interest Boundaries for Manual Segmentation.** Definitions of the region of interest boundaries used during the manual segmentation process within ITK-SNAP 3.8.0. These definitions were adopted from and very similar to a previous paper by Linderup et al. 2015.

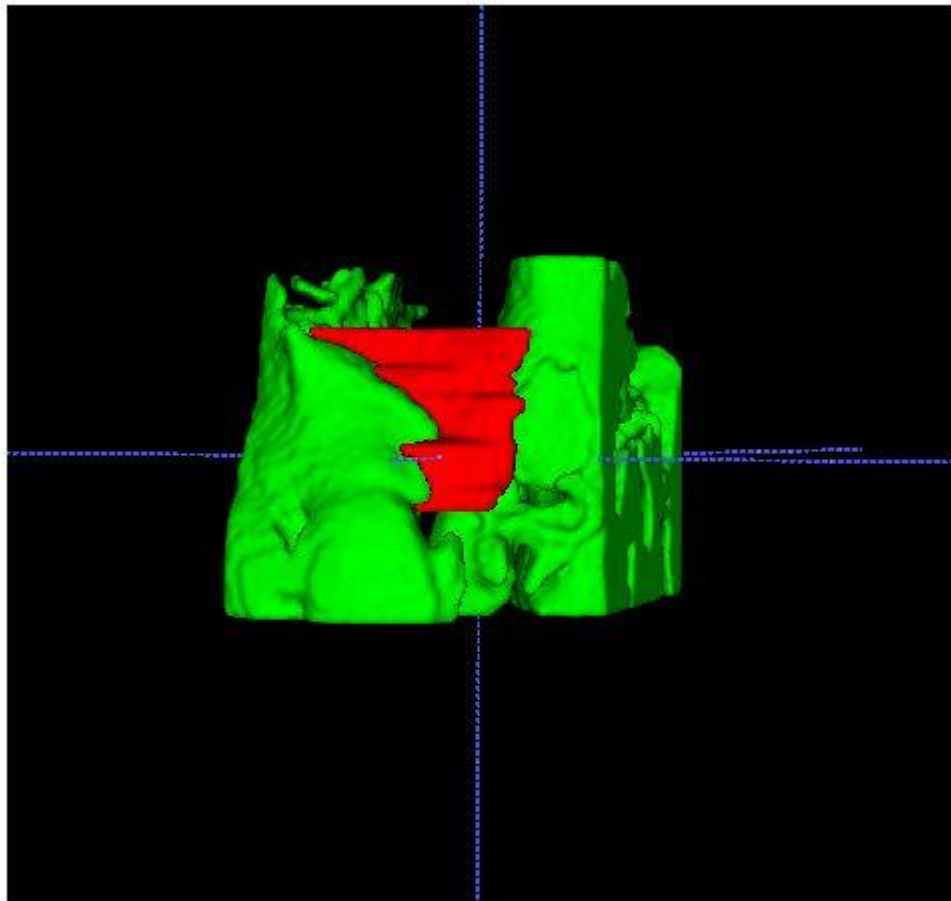
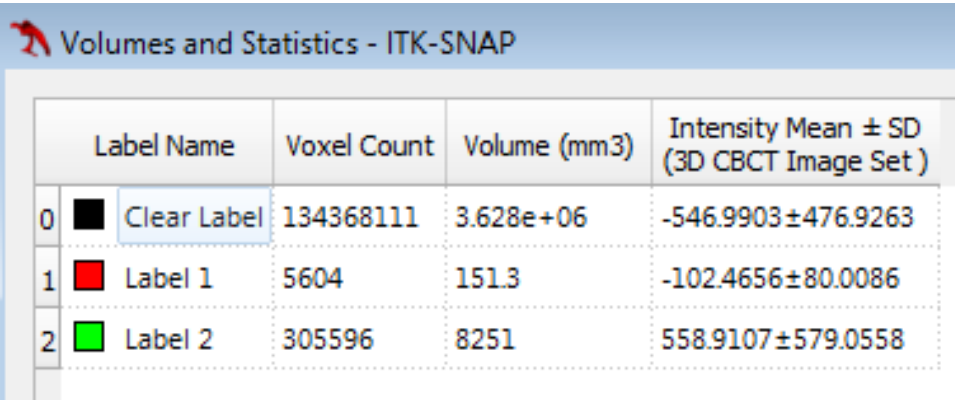


**Figure 4.3.6: Final Volumetric Segmentation Image in ITK-SNAP 3.8.0.** Example of a left side unilateral alveolar cleft segmented in ITK-SNAP 3.8.0. software for final analysis. *Green:* bone and/or hard tissues *Red:* soft tissues representing the alveolar cleft defect. Note the “tornado” shape of this pyramidal cleft defect.



	Label Name	Voxel Count	Volume (mm3)	Intensity Mean $\pm$ SD (3D CBCT Image Set)
0	Clear Label	1343681111	3.628e+06	-546.9903 $\pm$ 476.9263
1	Label 1	5604	151.3	-102.4656 $\pm$ 80.0086
2	Label 2	305596	8251	558.9107 $\pm$ 579.0558

**Figure 4.3.7: Final Volumetric Measurement in ITK-SNAP 3.8.0.** “Volumes and Statistics” tab within ITK-SNAP 3.8.0. *Green*: bone and/or hard tissue volume segmented *Red*: soft tissue representing the cleft defect segmented. These values were recorded in an excel file for final analysis.

## CHAPTER 5: RESULTS

### 5.1. Subjects

The records of all the patients who have received secondary alveolar bone grafts at the University of Nebraska Medical Center Oral and Maxillofacial Surgery Center from June 1, 2014 to January 1, 2020 were retrieved. Twenty four patients were included in this study after application of the exclusion and inclusion criteria and their pre-graft and 6-month post-graft CBCT scans were analyzed. Of the 24 patients, one was excluded as the graft surgery was deemed a failure. Data collected from 23 patients were submitted for statistical analysis. The average age of the patients in this study was 10 years 3 months (range = 8-13 years; SD = 1 year 6 months). Of the 23 patients included, 12 were female and 11 were male. There were 13 left-sided unilateral alveolar clefts and 10 right-sided unilateral alveolar clefts.

### 5.2. Demographic Variables and Their Effects on Outcomes

#### 5.2.1. Gender

The effect of gender on the alveolar bone graft outcomes was evaluated. Figure 5.2.1.1 displays the raw percent residual defect reported for male and female patients. When analyzing percent residual defect using a generalized linear model (GLM) following a beta distribution with a logit link function, Table 5.2.1.1 shows that there is a statistically significant difference in the true mean percent residual defect between males and females ( $F=10.63$ ;  $DF=1,21$ ;  $p=0.0037$ ).

The least square means for the mean percent residual defect by male and female can be viewed in Table 5.2.1.2. The estimated mean percent residual defect for females is 20.52% (Standard Error = 4.2%) and we are 95% confident the true mean percent residual defect for females is between 13.1% and 30.68%. The estimated mean percent residual defect for males is 44.20% (Standard Error = 5.7%) and we are 95% confident the true mean percent residual defect

for males is between 32.93% and 56.1%. This information can also be reported and visualized in a plot with error bars indicating the 95% confidence interval (Figure 5.2.1.2).

### **5.2.2. Age of the Patient at the Time of Grafting**

Age of the patient at the time of grafting was evaluated to determine if it had an effect on alveolar bone graft outcomes. Figure 5.2.2.1 displays the raw percent residual defect reported for age of patient at the time of grafting. When analyzing percent residual defect using a GLM following a beta distribution with a logit link function, Table 5.2.2.1 shows that there is no statistically significant relationship between the percent residual defect and the age of the patient at the time of grafting ( $F=0.00$ ;  $DF=1,21$ ;  $p=0.97$ ).

The regression coefficient estimates for the intercept, age of the patient at the time of grafting, and residual variance (scale) can be viewed in Table 5.2.2.2. Note that these estimates are on the model scale (non-normal data distribution) and will not have a direct interpretation other than direction of the slope. For percent residual defect and age of the patient at the time of grafting, the estimated slope is negative with a value of  $-0.00466$  (standard error =  $0.1297$ ).

### **5.2.3. Side of the Alveolar Cleft**

The effect of side of the alveolar cleft on the alveolar bone graft outcomes was evaluated. Figure 5.2.3.1 displays the raw percent residual defect reported for left and right side alveolar clefts. When analyzing percent residual defect using a GLM following a beta distribution with a logit link function, Table 5.2.3.1 shows that there is no statistically significant difference in the true mean percent residual defect between left and right side alveolar clefts ( $F=0.6$ ;  $DF=1,21$ ;  $p=0.45$ ).

The least square means for the mean percent residual defect by left and right side alveolar clefts can be viewed in Table 5.2.3.2. The estimated mean percent residual defect for the left side alveolar cleft is 34.46% (Standard Error = 5.7%) and we are 95% confident the true mean percent

residual defect for left side alveolar cleft is between 23.67% and 47.12%. The estimated mean percent residual defect for the right side alveolar cleft is 28.06% (Standard Error = 6.0%) and we are 95% confident the true mean percent residual defect for right side alveolar cleft is between 17.31% and 42.08%. This information can also be reported and visualized in a plot with error bars indicating the 95% confidence interval (Figure 5.2.3.2).

### **5.3. Linear Values and Their Effects on Outcomes**

#### **5.3.1. Cleft Side Canine Root Length**

Root length of the canine on the alveolar cleft side was measured to determine if it had an effect on the outcome of the alveolar bone grafts. The lengths were compared to previously reported mature maxillary canine root length values and analyzed as a percent. Figure 5.3.1.1 displays the raw percent residual defect reported for the cleft side canine root length percent. When analyzing percent residual defect using a GLM following a beta distribution with a logit link function, Table 5.3.1.1 shows that there is no statistically significant relationship between the percent residual defect and cleft side canine root length percent ( $F=0.61$ ;  $DF=1,21$ ;  $p=0.44$ ).

The regression coefficient estimates for the intercept, cleft side canine root length percent, and residual variance (scale) can be viewed in Table 5.3.1.2. Note that these estimates are on the model scale (non-normal data distribution) and will not have a direct interpretation other than direction of the slope. For residual defect and percent root length of the canine on the cleft side, the estimated slope is negative with a value of  $-0.9491$  (standard error = 1.22).

#### **5.3.2. Cleft Side Canine Angulation; Coronal Section**

Angulation, in the coronal section, of the canine on the alveolar cleft side was measured to determine if it had an effect on the outcome of the secondary alveolar bone graft. Figure 5.3.2.1 displays the raw percent residual defect reported for the cleft side canine angulation in the coronal section. Even though there is a slight upward trend, this was not statistically significant.

When analyzing percent residual defect using a GLM following a beta distribution with logit link function, Table 5.3.2.1 shows that there is no statistically significant relationship between the percent residual defect and cleft side canine angulation in the coronal section ( $F=2.15$ ;  $DF=1,21$ ;  $p=0.15$ ).

The regression coefficient estimates for the intercept, angulation of the canine on the cleft side in the coronal section, and residual variance (scale) can be viewed in Table 5.3.2.2. Note that these estimates are on the model scale (non-normal data distribution) and will not have a direct interpretation other than direction of the slope. For residual defect and angulation of the canine on the alveolar cleft side in the coronal section, the estimated slope is positive with a value of 0.03561 (standard error = 0.024).

### **5.3.3. Cleft side Canine Angulation; Sagittal Section**

Angulation, in the sagittal section, of the canine on the alveolar cleft side was measured to determine if it had an effect on the outcome of the secondary alveolar bone graft. Figure 5.3.3.1 displays the raw percent residual defect reported for the cleft side canine angulation in the sagittal section. Even though there is a slight downward trend, this was not statistically significant. When analyzing percent residual defect using GLM following a beta distribution with logit link function, Table 5.3.3.1 shows that there is no statistically significant relationship between the percent residual defect and angulation of the canine on the cleft side in the sagittal section ( $F=0.13$ ;  $DF=1,21$ ;  $p=0.72$ ).

The regression coefficient estimates for the intercept, angulation of the canine on the cleft side in the sagittal section, and residual variance (scale) can be viewed in Table 5.3.3.2. Note that these estimates are on the model scale (non-normal data distribution) and will not have a direct interpretation other than direction of the slope. For residual defect and angulation of the canine on the alveolar cleft side in the sagittal section, the estimated slope is negative with a value of -0.00592 (standard error = 0.016).

#### **5.3.4. Cleft Side Canine Distance from the Occlusal Plane**

Distance of the canine on the alveolar cleft side from the occlusal plane was measured to determine if it had an effect on the outcome of the secondary alveolar bone graft. Figure 5.3.4.1 displays the raw percent residual defect reported for the cleft side canine distance from the occlusal plane. When analyzing percent residual defect using GLM following a beta distribution with logit link function, Table 5.3.4.1 shows that there is no statistically significant relationship between the percent residual defect and distance of the canine on the cleft side from the occlusal plane ( $F=0.11$ ;  $DF=1,21$ ;  $p=0.74$ ).

The regression coefficient estimates for the intercept, cleft side canine distance from the occlusal plane, and residual variance (scale) can be viewed in Table 5.3.4.2. Note that these estimates are on the model scale (non-normal data distribution) and will not have a direct interpretation other than direction of the slope. For residual defect and distance of the canine on the alveolar cleft side from the occlusal plane, the estimated slope is positive with a value of 0.01404 (standard error = 0.042).

#### **5.4. Volumetric Values and Percent Residual Defect**

Volume of the clefts were measured to determine the overall success rate of using rhBMP-2 as a grafting material during secondary alveolar bone grafts. Pre-graft and 6-month post-graft CBCT images were analyzed for the 23 patients. Table 5.4.1 displays the observed cleft volumes (in  $\text{mm}^3$ ) for the subjects included in this study. Overall, the mean pre-graft volume of the unilateral cleft was 1026.97 (SD = 390.11) and the mean post-graft volume of the unilateral cleft was 333.48 (SD = 250.94). Table 5.4.1 also outlines the mean volume values for male/female and left/right side alveolar cleft. This information is also represented in a box & whisker plot with the inner quartile range displayed (Figure 5.4.1).

To report the success rates of secondary alveolar bone grafts, we reported our measurements as a percent residual defect calculated from the pre-graft and post-graft CBCT



scans. Overall, the mean percent residual defect was 0.32 (32%) (SD = 0.22) meaning a percent bone fill value of 0.68 (68%) following the procedure. These values, along with average percent residual defect values for male/female and left/right side alveolar clefts can be seen in Table 5.4.2. This information is also represented in box and whisker plots with the inner quartile range displayed (Figures 5.4.2, 5.4.3, and 5.4.4).

### **5.5. Intra-examiner and Inter-examiner Reliability**

Intraclass correlations were used to measure intra-examiner and inter-examiner values throughout this study. The intraclass correlations-3 (ICC3) was the value analyzed. This value is used when all subjects are rated by the same raters who are assumed to be the entire population of raters (Shrout and Fleiss 1979). For this study, the ICC3 values ranged from 0.72 to 1.0 representing a moderate to excellent correlation between the investigators. A general guideline for ICC values is: below 0.50 (poor), between 0.50 and 0.75 (moderate), between 0.75 and 0.90 (good), and above 0.90 (excellent).

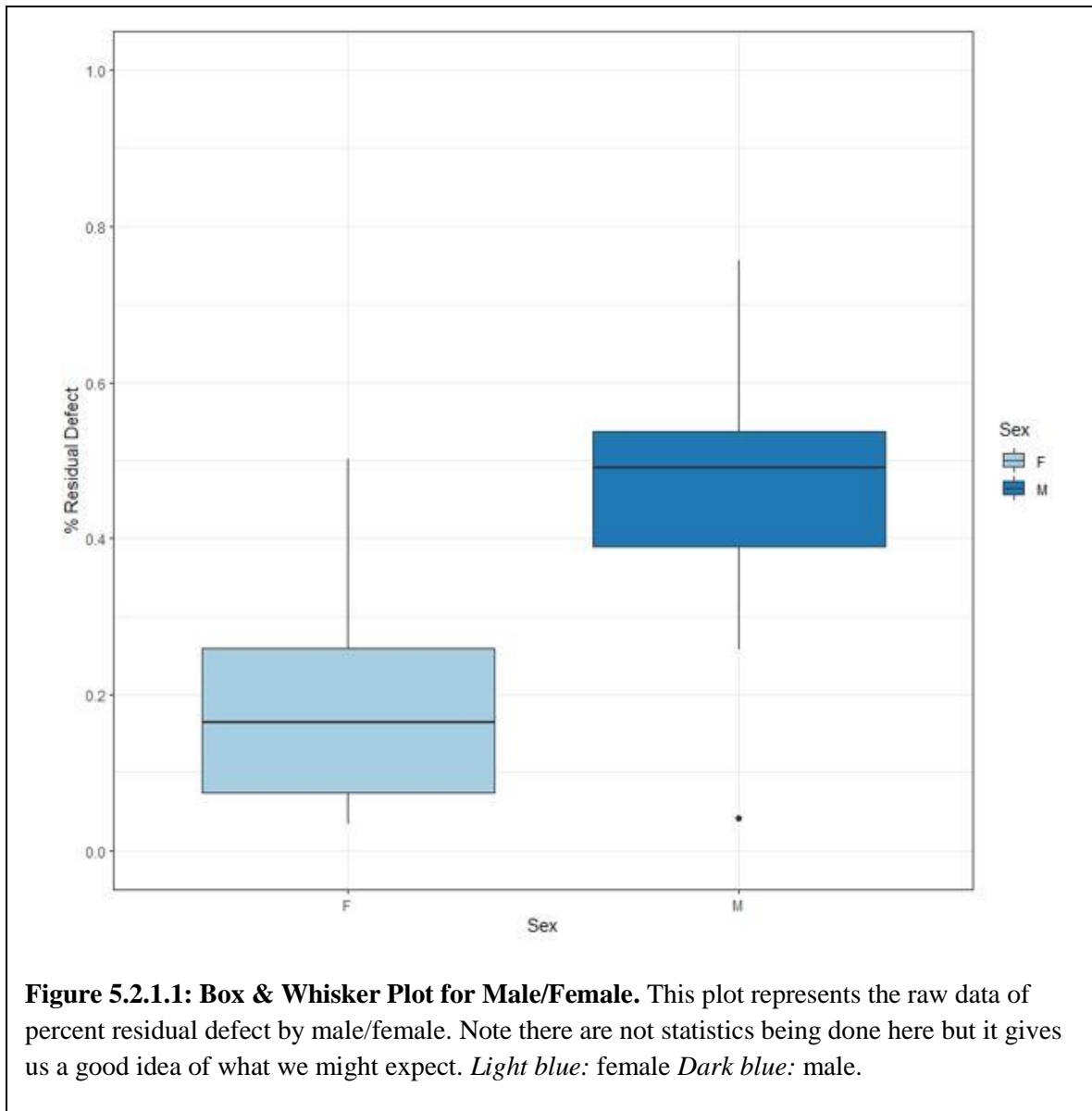
Table 5.5.1 displays the volumes of the unilateral alveolar clefts. 20 pre-graft and post-graft CBCT images were analyzed by investigator LP and SP independently. The ICC3 value for the inter-examiner reliability for the volumes of the cleft was 0.99 (F=167; DF=19,19; p<0.0001). These results are represented in Table 5.5.2.

Tables 5.5.3 and 5.5.4 display the intra-examiner results for the volumes measured (by investigators LP and SP) for the unilateral alveolar clefts. The ICC3 value for investigator LP was 1.0 (F=746; DF=19,19; p<0.0001). The ICC3 value for investigator SP was also 1.0 (F=1025; DF=19,19; p<0.0001).

The inter-examiner reliability for the length of the canine on the cleft side can be seen in Table 5.5.5. The ICC3 value for inter-examiner reliability length of the canine on the cleft side was 0.72 (F=6.1; DF=19,19; p<0.001).

Tables 5.5.6 and 5.5.7 display the intra-examiner results for the length of the canine on the cleft side, measured by investigators LP and SP. The ICC3 value for investigator LP was 0.94 (F=34; DF=19,19;  $p<0.0001$ ). The ICC3 value for investigator SP was 0.94 (F=32; DF=19,19;  $p<0.0001$ ).

Angulation, in both the coronal and sagittal sections, of the canine on the alveolar cleft side as well as the distance of the canine on the alveolar cleft side from the occlusal plane was only measured by investigator LP. Intra-examiner reliability was calculated for these values and can be seen in Tables 5.5.8, 5.5.9, and 5.5.10. The ICC3 value for the angulation of the canine on the cleft side in the coronal section was 0.95 (F=41; DF=19,19;  $p<0.0001$ ). The ICC3 value for the angulation of the canine on the cleft side in the sagittal section was 0.99 (F=180; DF=19,19;  $p<0.0001$ ). And finally, the ICC3 value for the distance of the canine on the cleft side from the occlusal plane was 1.0 (F=458; DF=19,19;  $p<0.0001$ ).

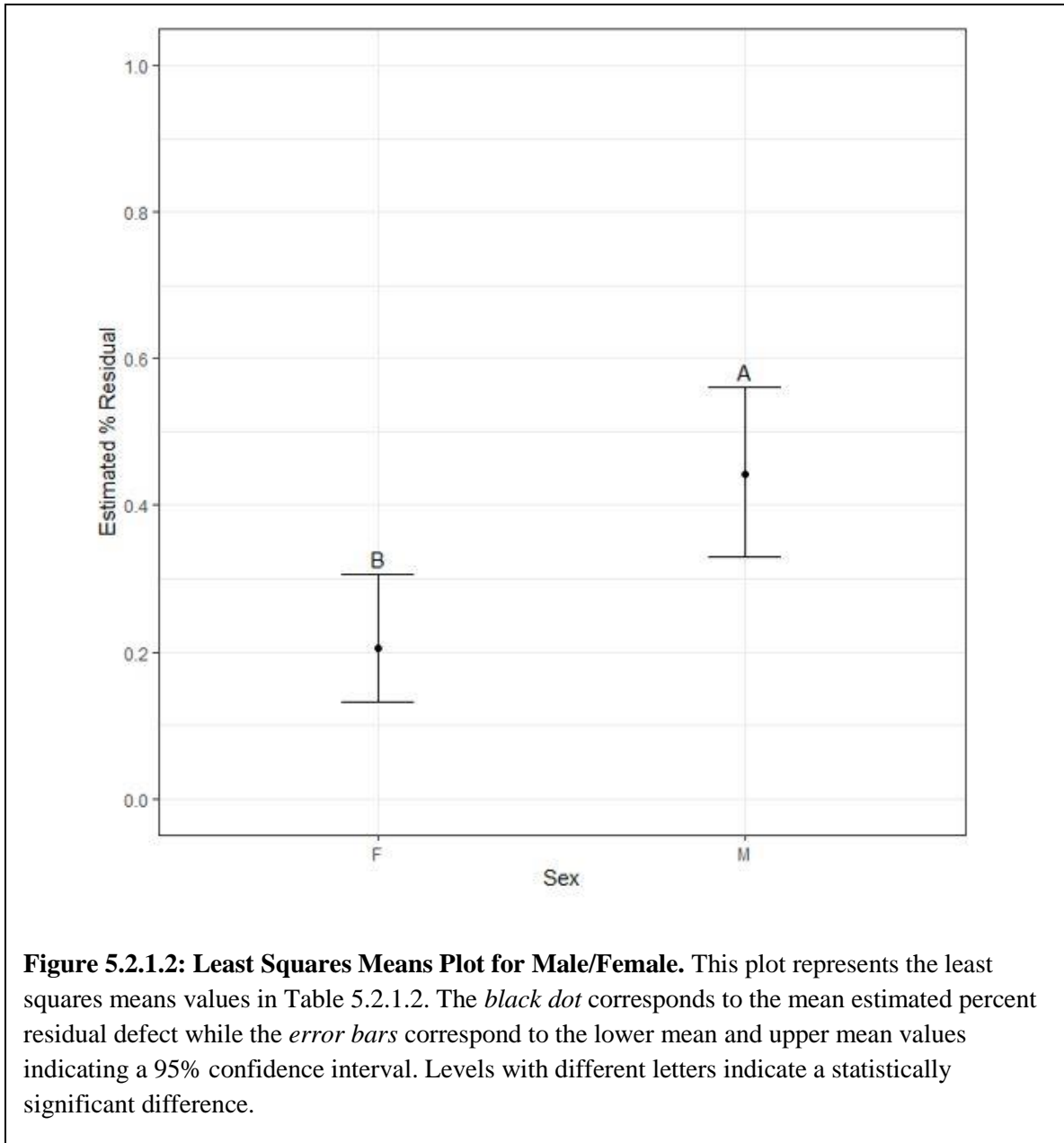


<b>Type III Tests of Fixed Effects</b>				
<b>Effect</b>	<b>Num DF</b>	<b>Den DF</b>	<b>F Value</b>	<b>Pr &gt; F</b>
<b>Sex</b>	1	21	10.63	0.0037

**Table 5.2.1.1: Type III Tests for Fixed Effects – Male/Female.** This table analyzes the percent residual defect by male/female using a generalized linear model following a beta distribution. A statistically significant difference was noticed in the true mean percent residual defect between males and females.

<b>Sex Least Squares Means</b>								
<b>Sex</b>	<b>DF</b>	<b>t Value</b>	<b>Pr &gt;  t </b>	<b>Alpha</b>	<b>Mean</b>	<b>Standard Error Mean</b>	<b>Lower Mean</b>	<b>Upper Mean</b>
<b>F</b>	21	-5.23	<.0001	0.05	0.2052	0.04225	0.1310	0.3068
<b>M</b>	21	-1.01	0.3222	0.05	0.4420	0.05671	0.3293	0.5610

**Table 5.2.1.2: Least Squares Means – Male/Female.** This table provides the least squares means for the mean percent residual defect by male and female. Calculations were made using the beta distribution and accounting for the variance estimated by the model.



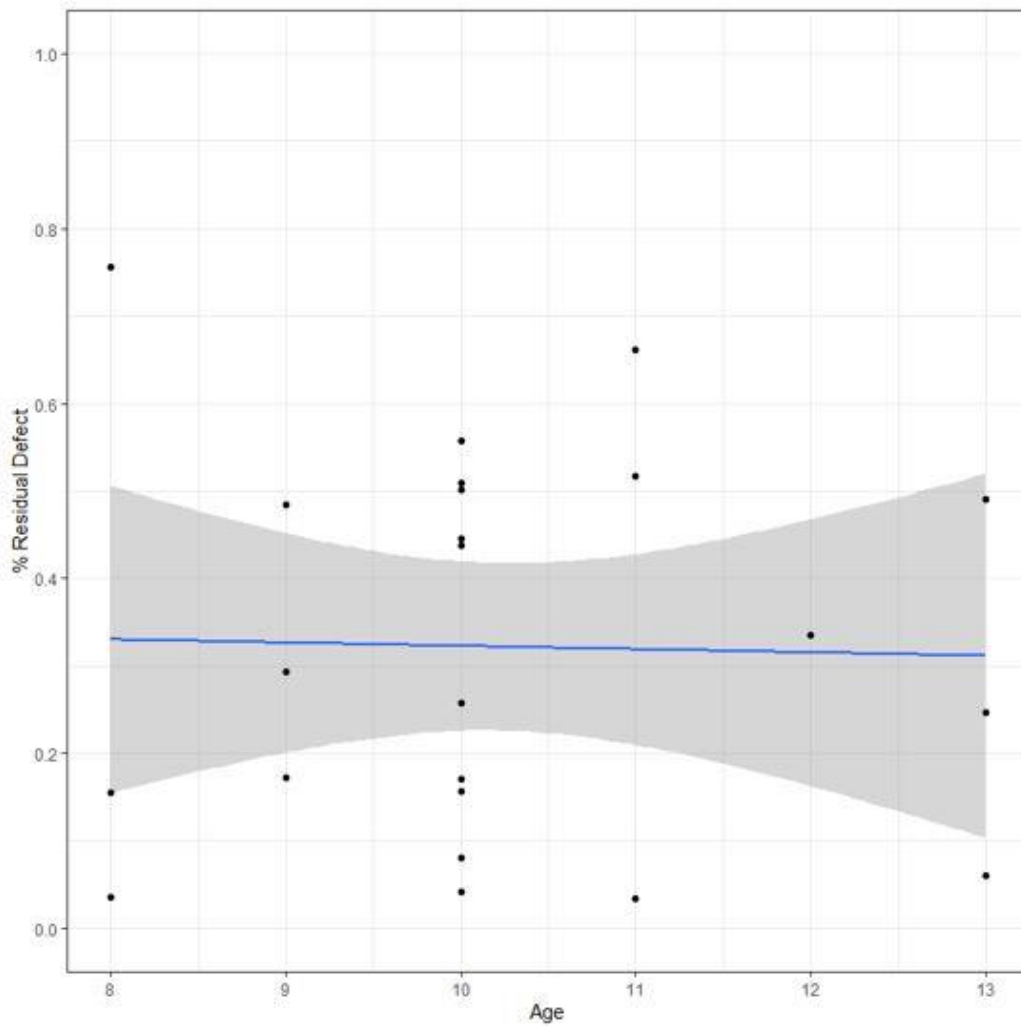


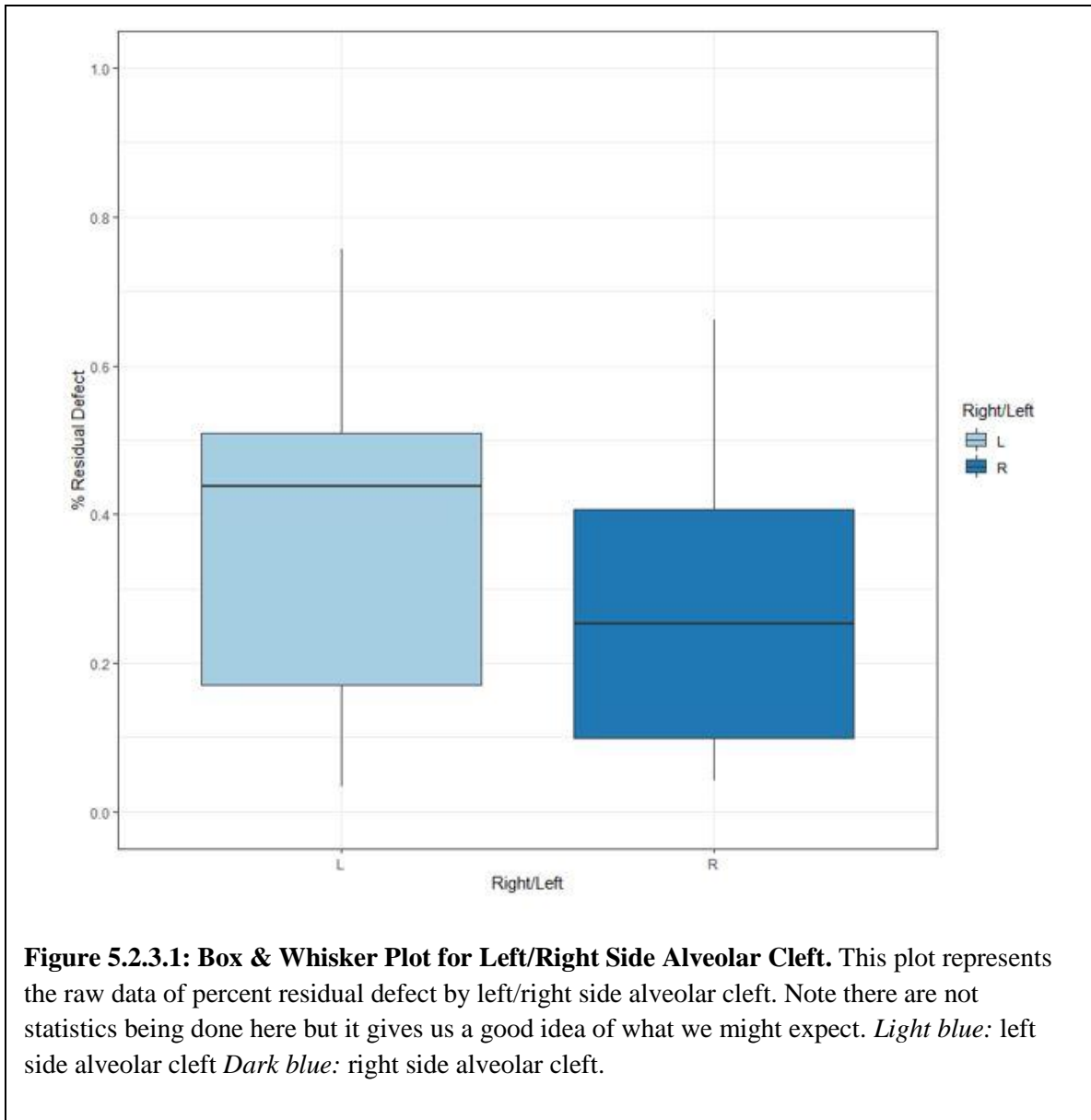
**Figure 5.2.2.1: Scatter Plot – Age of Patient at Time of Grafting.** This scatter plot displays the raw percent residual defect by age. The ages are represented as a quantitative/numeric value. The *blue line* represents a linear regression line to provide an idea of whether we are seeing a trend or not. The *shaded area* represents the 95% confidence interval. Note there are not statistics being done here.

<b>Type I Tests of Fixed Effects</b>				
<b>Effect</b>	<b>Num DF</b>	<b>Den DF</b>	<b>F Value</b>	<b>Pr &gt; F</b>
<b>Age</b>	1	21	0.00	0.9717

**Table 5.2.2.1: Type I Tests of Fixed Effects - Age.** This table analyzes the percent residual defect by patient age at the time of grafting by using a generalized linear model following a beta distribution. No statistically significant relationship between the percent residual defect and the age of the patient was noticed.

<b>Parameter Estimates</b>					
<b>Effect</b>	<b>Estimate</b>	<b>Standard Error</b>	<b>DF</b>	<b>t Value</b>	<b>Pr &gt;  t </b>
<b>Intercept</b>	-0.7221	1.3403	21	-0.54	0.5957
<b>Age</b>	-0.00466	0.1297	21	-0.04	0.9717
<b>Scale</b>	3.9017	1.0598	.	.	.

**Table 5.2.2.2: Regression Coefficient Estimates for Age of the Patient.** This table displays the regression coefficient estimates for the intercept, age of the patient at the time of grafting, and residual variance (scale). These estimates are on a model scale so will not have a direct interpretation other than the direction of the estimated slope (negative).



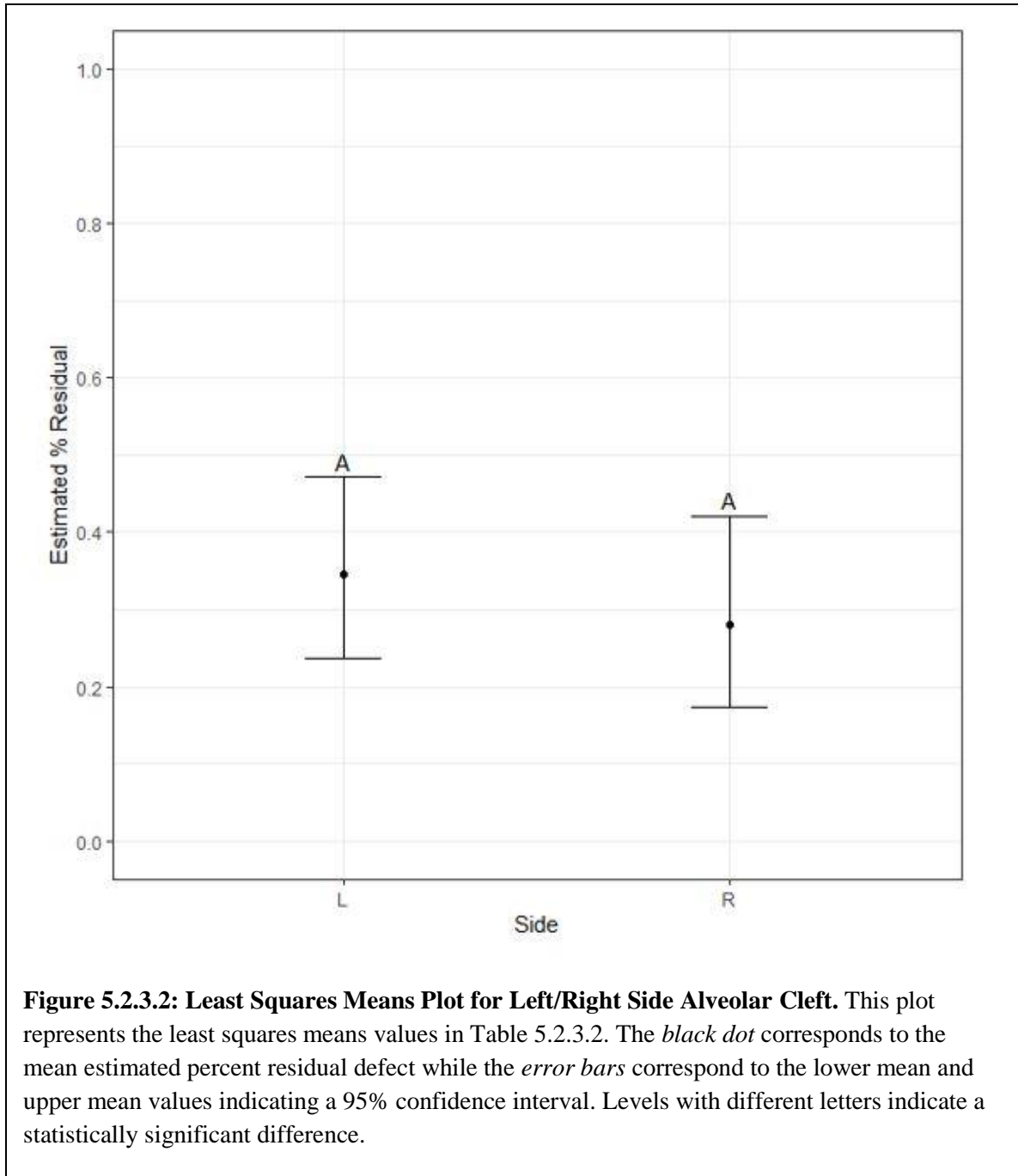


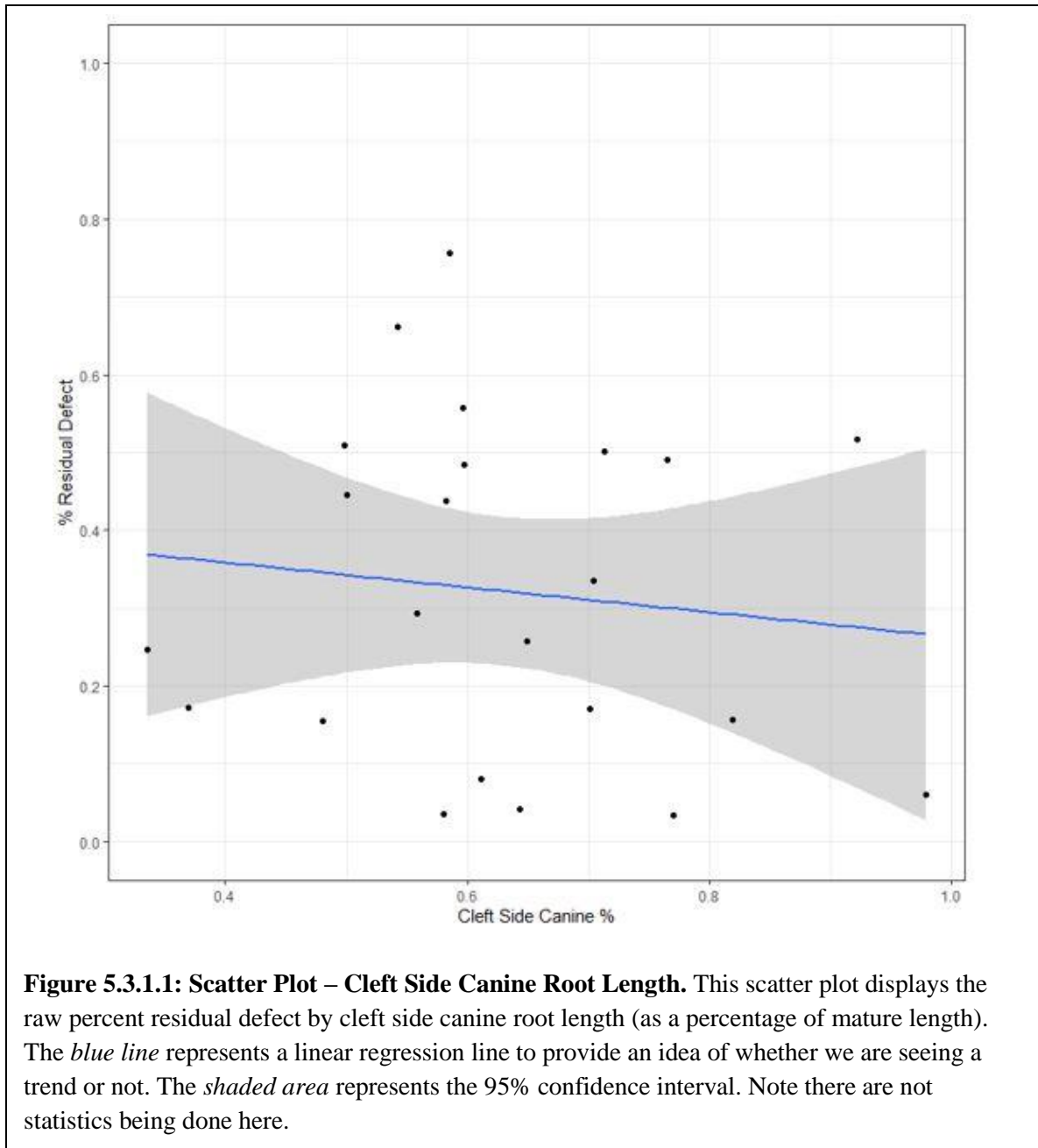
<b>Type III Tests of Fixed Effects</b>				
<b>Effect</b>	<b>Num DF</b>	<b>Den DF</b>	<b>F Value</b>	<b>Pr &gt; F</b>
<b>Right Left</b>	1	21	0.60	0.4455

**Table 5.2.3.1: Type III Tests for Fixed Effects – Left/Right Side Alveolar Cleft.** This table analyzes the percent residual defect by left/right side cleft using a generalized linear model following a beta distribution. No statistically significant difference was noticed in the true mean percent residual defect between left and right side alveolar clefts.

<b>Right Left Least Squares Means</b>								
<b>Right Left</b>	<b>DF</b>	<b>t Value</b>	<b>Pr &gt;  t </b>	<b>Alpha</b>	<b>Mean</b>	<b>Standard Error Mean</b>	<b>Lower Mean</b>	<b>Upper Mean</b>
<b>L</b>	21	-2.53	0.0193	0.05	0.3446	0.05731	0.2367	0.4712
<b>R</b>	21	-3.15	0.0049	0.05	0.2806	0.06039	0.1731	0.4208

**Table 5.2.3.2: Least Squares Means – Left/Right Side Alveolar Cleft.** This table provides the least squares means for the mean percent residual defect by left/right side cleft. Calculations were made using the beta distribution and accounting for the variance estimated by the model.





Type I Tests of Fixed Effects				
Effect	Num DF	Den DF	F Value	Pr > F
<u>Cleft Side Canine</u>	1	21	0.61	0.4448

**Table 5.3.1.1: Type I Tests of Fixed Effects – Cleft Side Canine Root Length.** This table analyzes the percent residual defect by cleft side canine root length using a generalized linear model following a beta distribution. No statistically significant relationship was noticed between the percent residual defect and the canine root length on the alveolar cleft side.

Parameter Estimates					
Effect	Estimate	Standard Error	DF	t Value	Pr >  t
<b>Intercept</b>	-0.1732	0.7889	21	-0.22	0.8284
<u>Cleft Side Canine</u>	-0.9491	1.2188	21	-0.78	0.4448
<b>Scale</b>	4.0063	1.0908	.	.	.

**Table 5.3.1.2: Regression Coefficient Estimates for Cleft Side Canine Root Length.** This table displays the regression coefficient estimates for the intercept, cleft side canine root length, and residual variance (scale). These estimates are on a model scale so will not have a direct interpretation other than the direction of the estimated slope (negative).

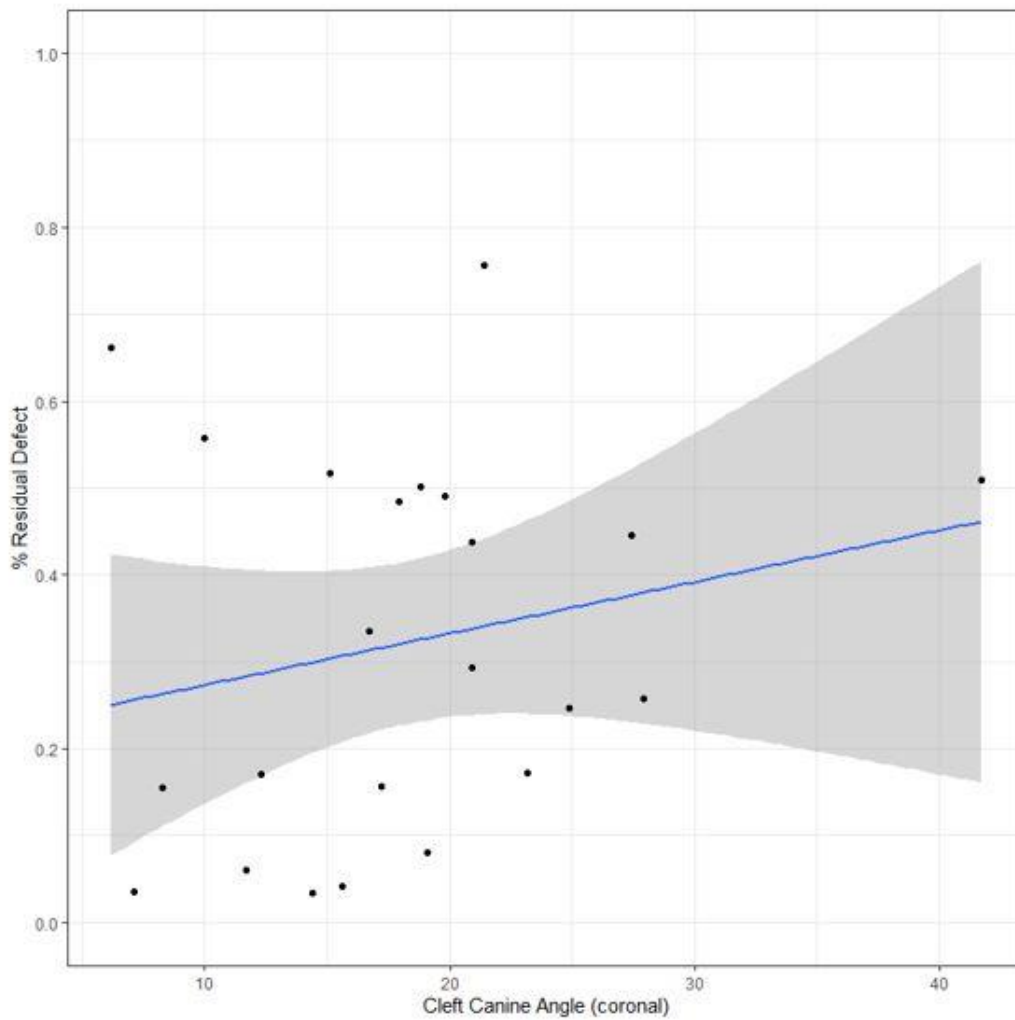


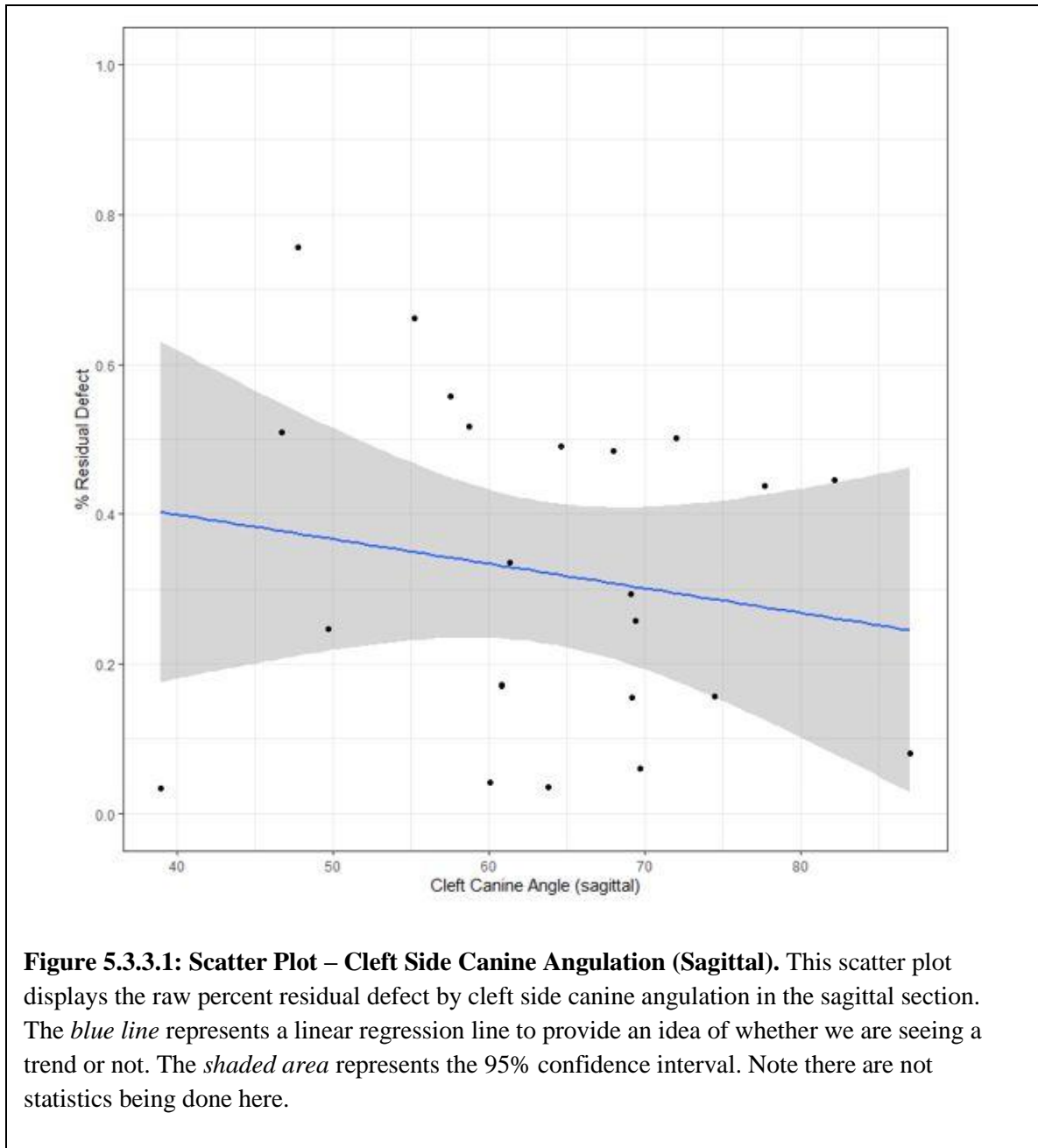
**Figure 5.3.2.1: Scatter Plot – Cleft Side Canine Angulation (Coronal).** This scatter plot displays the raw percent residual defect by cleft side canine angulation in the coronal section. The *blue line* represents a linear regression line to provide an idea of whether we are seeing a trend or not. The *shaded area* represents the 95% confidence interval. Note there are not statistics being done here.

<b>Type I Tests of Fixed Effects</b>				
<b>Effect</b>	<b>Num DF</b>	<b>Den DF</b>	<b>F Value</b>	<b>Pr &gt; F</b>
<b>Cleft Canine Angle</b>	1	21	2.15	0.1576

**Table 5.3.2.1: Type I Tests of Fixed Effects – Cleft Side Canine Angulation (Coronal).** This table analyzes the percent residual defect by cleft side canine angulation in the coronal section using a generalized linear model following a beta distribution. No statistically significant relationship was noticed between the percent residual defect and the cleft side canine angulation when viewed in the coronal section.

<b>Parameter Estimates</b>					
<b>Effect</b>	<b>Estimate</b>	<b>Standard Error</b>	<b>DF</b>	<b>t Value</b>	<b>Pr &gt;  t </b>
<b>Intercept</b>	-1.4301	0.4945	21	-2.89	0.0087
<b>Cleft Canine Angle</b>	0.03561	0.02430	21	1.47	0.1576
<b>Scale</b>	4.2827	1.1743	.	.	.

**Table 5.3.2.2: Regression Coefficient Estimates for Cleft Side Canine Angulation (Coronal).** This table displays the regression coefficient estimates for the intercept, cleft side canine angulation in the coronal section, and residual variance (scale). These estimates are on a model scale so will not have a direct interpretation other than the direction of the estimated slope (positive).



<b>Type I Tests of Fixed Effects</b>				
<b>Effect</b>	<b>Num DF</b>	<b>Den DF</b>	<b>F Value</b>	<b>Pr &gt; F</b>
<b>Cleft Canine Angle</b>	1	21	0.13	0.7210

**Table 5.3.3.1: Type I Tests of Fixed Effects – Cleft Side Canine Angulation (Sagittal).** This table analyzes the percent residual defect by cleft side canine angulation in the sagittal section using a generalized linear model following a beta distribution. No statistically significant relationship was noticed between the percent residual defect and the cleft side canine angulation when viewed in the sagittal section.

<b>Parameter Estimates</b>					
<b>Effect</b>	<b>Estimate</b>	<b>Standard Error</b>	<b>DF</b>	<b>t Value</b>	<b>Pr &gt;  t </b>
<b>Intercept</b>	-0.3934	1.0575	21	-0.37	0.7136
<b>Cleft Canine Angle</b>	-0.00592	0.01634	21	-0.36	0.7210
<b>Scale</b>	3.9238	1.0663	.	.	.

**Table 5.3.3.2: Regression Coefficient Estimates for Cleft Side Canine Angulation (Sagittal).** This table displays the regression coefficient estimates for the intercept, cleft side canine angulation in the sagittal section, and residual variance (scale). These estimates are on a model scale so will not have a direct interpretation other than the direction of the estimated slope (negative).



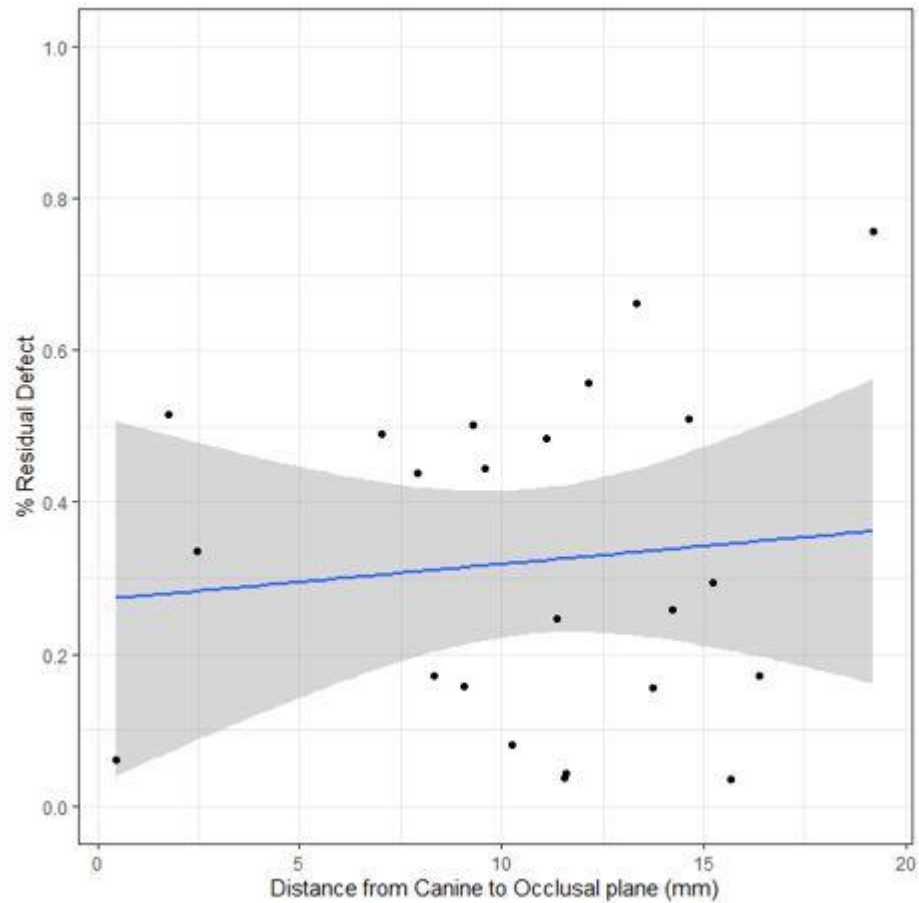


**Figure 5.3.4.1: Scatter Plot – Cleft Side Canine Distance from Occlusal Plane.** This scatter plot displays the raw percent residual defect by cleft side canine distance from occlusal plane. The *blue line* represents a linear regression line to provide an idea of whether we are seeing a trend or not. The *shaded area* represents the 95% confidence interval. Note there are not statistics being done here.

<b>Type I Tests of Fixed Effects</b>				
<b>Effect</b>	<b>Num DF</b>	<b>Den DF</b>	<b>F Value</b>	<b>Pr &gt; F</b>
<b>Distance from Canine</b>	1	21	0.11	0.7443

**Table 5.3.4.1: Type I Tests of Fixed Effects – Cleft Side Canine Distance from Occlusal Plane.** This table analyzes the percent residual defect by cleft side canine distance from the occlusal plane using a generalized linear model following a beta distribution. No statistically significant relationship was noticed between the percent residual defect and the cleft side canine distance.

<b>Parameter Estimates</b>					
<b>Effect</b>	<b>Estimate</b>	<b>Standard Error</b>	<b>DF</b>	<b>t Value</b>	<b>Pr &gt;  t </b>
<b>Intercept</b>	-0.9207	0.5001	21	-1.84	0.0798
<b>Distance from Canine</b>	0.01404	0.04247	21	0.33	0.7443
<b>Scale</b>	3.9210	1.0657	.	.	.

**Table 5.3.4.2: Regression Coefficient Estimates for Cleft Side Canine Distance from Occlusal Plane.** This table displays the regression coefficient estimates for the intercept, cleft side canine distance from occlusal plane, and residual variance (scale). These estimates are on a model scale so will not have a direct interpretation other than the direction of the estimated slope (positive).

		Volumetric Value (mm <sup>3</sup> )			
<u>Pre</u>	<u>Post</u>	<u>Scan</u>	<u>N Obs</u>	<u>Mean</u>	<u>Std Dev</u>
<b>Post</b>	<b>Overall</b>		<b>23</b>	333.48	250.94
<b>Pre</b>	<b>Overall</b>		<b>23</b>	1026.97	390.11
<b>Post</b>	<b>Female</b>		<b>12</b>	198.27	179.17
	<b>Male</b>		<b>11</b>	480.97	239.51
<b>Pre</b>	<b>Female</b>		<b>12</b>	998.07	315.31
	<b>Male</b>		<b>11</b>	1058.49	472.59
<b>Post</b>	<b>Left</b>		<b>13</b>	410.3	272.67
	<b>Right</b>		<b>10</b>	233.6	187.61
<b>Pre</b>	<b>Left</b>		<b>13</b>	1159.68	442.0
	<b>Right</b>		<b>10</b>	854.43	230.22

**Table 5.4.1: Overall Volumetric Values for Unilateral Clefts.** This table displays the overall volumetric values in mm<sup>3</sup> for the unilateral clefts. A total of 23 patients were included for the statistical analysis summary. Pre-graft and 6-month post-graft CBCT images were evaluated. The table also includes volumetric values for left/right alveolar cleft and male/female variables within our sample.

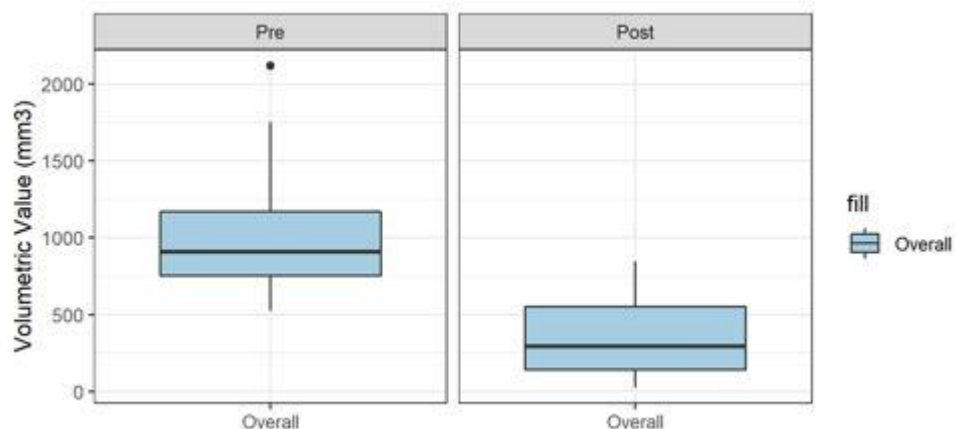


**Figure 5.4.1: Overall Volumetric Values for Unilateral Clefts.** This box & whisker plots display the overall volumetric values in mm<sup>3</sup> for the unilateral clefts. A total of 23 patients were included for the statistical analysis summary. Pre-graft (*left*) and 6-month post-graft (*right*) CBCT images were evaluated. *Black horizontal line*: 50<sup>th</sup> percentile (median) *Blue box*: inner quartile range (25<sup>th</sup> -75<sup>th</sup> percentile).

% Residual Defect			
	N Obs	Mean	Std Dev
<b>Overall</b>	<b>23</b>	0.32	0.22
<b>Female</b>	<b>12</b>	0.196	0.151
<b>Male</b>	<b>11</b>	0.46	0.19
<b>Left</b>	<b>13</b>	0.36	0.23
<b>Right</b>	<b>10</b>	0.27	0.21

**Table 5.4.2: Percent Residual Defect Using rhBMP-2.** This table shows the overall percent residual defect measured on the 6-month post-graft CBCT images for the 23 patients in our study. A mean value of 0.32 (SD = 0.22) represents a 32% residual defect in the post-graft scan meaning an overall bone fill of 68% using rhBMP-2 for secondary grafting of unilateral alveolar clefts. The table also includes the breakdown of percent residual defect for left/right alveolar cleft and male/female variables within our sample.

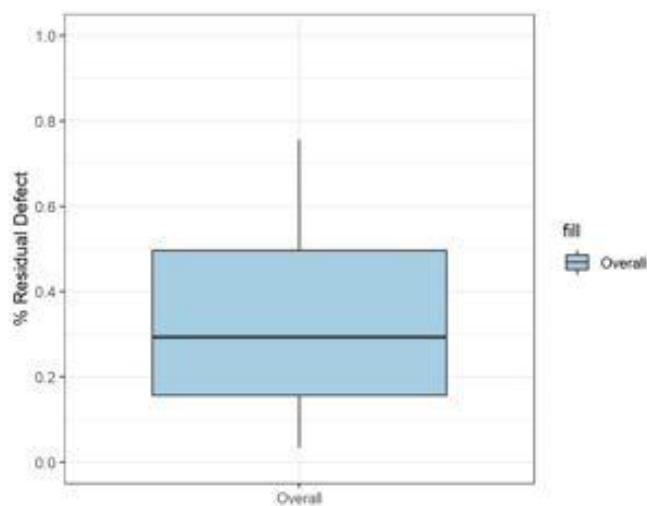


**Figure 5.4.2: Percent Residual Defect Using rhBMP-2.** This box & whisker plot displays the overall percent residual defect using rhBMP-2. A total of 23 patients were included for the statistical analysis summary. *Black horizontal line: 50<sup>th</sup> percentile (median) Blue box: inner quartile range (25<sup>th</sup> -75<sup>th</sup> percentile).*

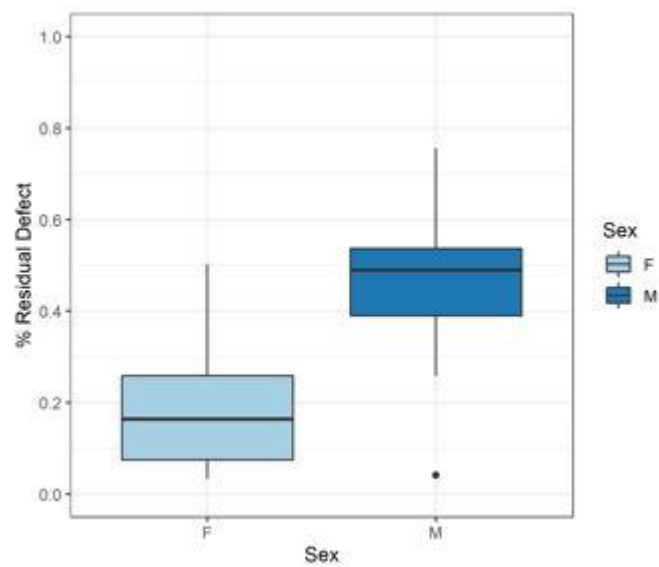


**Figure 5.4.3: Percent Residual Defect Using rhBMP-2; Male/Female.** This box & whisker plot displays the overall percent residual defect using rhBMP-2 for male/female patients. 11 males (*right*) and 12 females (*left*) were included for the statistical analysis summary. *Black horizontal lines:* 50<sup>th</sup> percentile (median) *Blue boxes:* inner quartile range (25<sup>th</sup> -75<sup>th</sup> percentile).

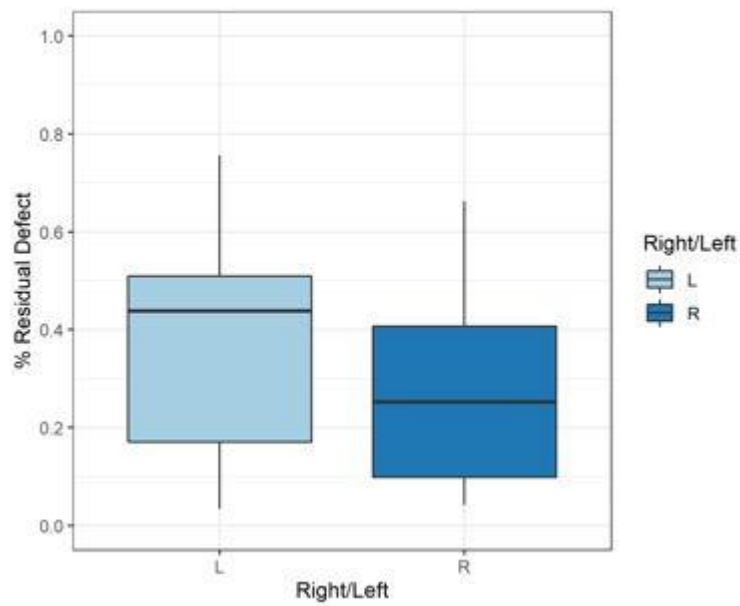


**Figure 5.4.4: Percent Residual Defect Using rhBMP-2; Left/Right Alveolar Cleft.** This box & whisker plot displays the overall percent residual defect using rhBMP-2 for left/right alveolar clefts. 13 left alveolar clefts (*left*) and 10 right alveolar clefts (*right*) were included for the statistical analysis summary. *Black horizontal lines:* 50<sup>th</sup> percentile (median) *Blue boxes:* inner quartile range (25<sup>th</sup> -75<sup>th</sup> percentile).

PatientID	Scan	ExaminerLP.T1	ExaminerSP.T1
1	Pre	805.30	748.90
1	Post	27.67	25.78
4	Pre	1093.00	972.40
4	Post	609.30	566.30
5	Pre	611.80	556.20
5	Post	307.00	302.70
6	Pre	1144.00	1168.00
6	Post	41.34	117.00
7	Pre	1111.00	1074.00
7	Post	566.10	499.80
8	Pre	885.50	929.28
8	Post	151.30	139.80
9	Pre	708.50	732.90
9	Post	56.56	58.37
10	Pre	908.50	882.70
10	Post	469.30	453.40
11	Pre	1471.00	1253.00
11	Post	230.50	279.40
15	Pre	1196.00	1158.00
15	Post	295.80	303.50

**Table 5.5.1: Inter-examiner Reliability Raw Data.** This table shows the volumetric values in mm<sup>3</sup> for the unilateral alveolar cleft on 10 patients included in this study. The 20 CBCT images (both pre-graft and post-graft) were measured independently by investigators LP and SP and submitted for statistical analysis.

```
## Intraclass correlation coefficients
##
##          type ICC  F df1 df2      p lower bound upper bound
## Single_raters_absolute ICC1 0.99 154 19 20 1.2e-17      0.97      0.99
## Single_random_raters   ICC2 0.99 167 19 19 3.3e-17      0.97      0.99
## Single_fixed_raters    ICC3 0.99 167 19 19 3.3e-17      0.97      0.99
## Average_raters_absolute ICC1k 0.99 154 19 20 1.2e-17      0.99      1.00
## Average_random_raters  ICC2k 0.99 167 19 19 3.3e-17      0.99      1.00
## Average_fixed_raters   ICC3k 0.99 167 19 19 3.3e-17      0.99      1.00
```

**Table 5.5.2: Inter-examiner ICC3 Results.** This table displays the inter-examiner intraclass correlation coefficients (ICC3) for unilateral cleft volume measured by investigators LP and SP. The results are based on 20 independently measured CBCT images. An ICC3 value of 0.99 represents excellent correlation.

## Intraclass correlation coefficients									
##	type	ICC	F	df1	df2	p	lower bound	upper bound	
## Single_raters_absolute	ICC1	1	693	19	20	4.1e-24	0.99		1
## Single_random_raters	ICC2	1	746	19	19	2.4e-23	0.99		1
## Single_fixed_raters	ICC3	1	746	19	19	2.4e-23	0.99		1
## Average_raters_absolute	ICC1k	1	693	19	20	4.1e-24	1.00		1
## Average_random_raters	ICC2k	1	746	19	19	2.4e-23	1.00		1
## Average_fixed_raters	ICC3k	1	746	19	19	2.4e-23	1.00		1

**Table 5.5.3: Intra-examiner ICC3 Results for Cleft Volume; Investigator LP.** This table displays the intra-examiner intraclass correlation coefficients (ICC3) for cleft volume. The results are based on initial 20 CBCT images measured by investigator LP. After at least 2 weeks, these same 10 patients (20 CBCT images) were analyzed by investigator LP. An ICC3 value of 1.0 represents excellent correlation.

## Intraclass correlation coefficients									
##	type	ICC	F	df1	df2	p	lower bound	upper bound	
## Single_raters_absolute	ICC1	1	1025	19	20	8.2e-26	1		1
## Single_random_raters	ICC2	1	1025	19	19	1.2e-24	1		1
## Single_fixed_raters	ICC3	1	1025	19	19	1.2e-24	1		1
## Average_raters_absolute	ICC1k	1	1025	19	20	8.2e-26	1		1
## Average_random_raters	ICC2k	1	1025	19	19	1.2e-24	1		1
## Average_fixed_raters	ICC3k	1	1025	19	19	1.2e-24	1		1

**Table 5.5.4: Intra-examiner ICC3 Results for Cleft Volume; Investigator SP.** This table displays the intra-examiner intraclass correlation coefficients (ICC3) for cleft volume. The results are based on initial 20 CBCT images measured by investigator SP. After at least 2 weeks, these same 10 patients (20 CBCT images) were analyzed by investigator SP. An ICC3 value of 1.0 represents excellent correlation.

## Intraclass correlation coefficients									
##	type	ICC	F	df1	df2	p	lower bound	upper bound	
## Single_raters_absolute	ICC1	0.72	6.1	19	20	8.5e-05	0.48		0.86
## Single_random_raters	ICC2	0.72	6.1	19	19	1.2e-04	0.48		0.86
## Single_fixed_raters	ICC3	0.72	6.1	19	19	1.2e-04	0.48		0.86
## Average_raters_absolute	ICC1k	0.84	6.1	19	20	8.5e-05	0.65		0.92
## Average_random_raters	ICC2k	0.84	6.1	19	19	1.2e-04	0.65		0.92
## Average_fixed_raters	ICC3k	0.84	6.1	19	19	1.2e-04	0.65		0.92

**Table 5.5.5: Inter-examiner ICC3 Results for Cleft Side Canine Length.** This table displays the inter-examiner intraclass correlation coefficients (ICC3) for cleft side canine length measured by investigators LP and SP. The results are based on 20 independently measured CBCT images. An ICC3 value of 0.72 is on the higher end of moderate correlation.



## Intraclass correlation coefficients									
##		type	ICC	F	df1	df2	p	lower bound	upper bound
##	Single_raters_absolute	ICC1	0.94	34	19	20	2.6e-11	0.88	0.97
##	Single_random_raters	ICC2	0.94	34	19	19	7.2e-11	0.88	0.97
##	Single_fixed_raters	ICC3	0.94	34	19	19	7.2e-11	0.88	0.97
##	Average_raters_absolute	ICC1k	0.97	34	19	20	2.6e-11	0.94	0.99
##	Average_random_raters	ICC2k	0.97	34	19	19	7.2e-11	0.94	0.99
##	Average_fixed_raters	ICC3k	0.97	34	19	19	7.2e-11	0.94	0.99

**Table 5.5.6: Intra-examiner ICC3 Results for Cleft Side Canine Length; Investigator LP.**

This table displays the intra-examiner intraclass correlation coefficients (ICC3) for cleft side canine length. The results are based on initial 20 CBCT images measured by investigator LP. After at least 2 weeks, these same 10 patients (20 CBCT images) were analyzed by investigator LP. An ICC3 value of 0.94 represents excellent correlation.

## Intraclass correlation coefficients									
##		type	ICC	F	df1	df2	p	lower bound	upper bound
##	Single_raters_absolute	ICC1	0.94	32	19	20	5.3e-11	0.87	0.97
##	Single_random_raters	ICC2	0.94	32	19	19	1.4e-10	0.87	0.97
##	Single_fixed_raters	ICC3	0.94	32	19	19	1.4e-10	0.87	0.97
##	Average_raters_absolute	ICC1k	0.97	32	19	20	5.3e-11	0.93	0.99
##	Average_random_raters	ICC2k	0.97	32	19	19	1.4e-10	0.93	0.99
##	Average_fixed_raters	ICC3k	0.97	32	19	19	1.4e-10	0.93	0.99

**Table 5.5.7: Intra-examiner ICC3 Results for Cleft Side Canine Length; Investigator SP.**

This table displays the intra-examiner intraclass correlation coefficients (ICC3) for cleft side canine length. The results are based on initial 20 CBCT images measured by investigator SP. After at least 2 weeks, these same 10 patients (20 CBCT images) were analyzed by investigator SP. An ICC3 value of 0.94 represents excellent correlation.

## Intraclass correlation coefficients									
##		type	ICC	F	df1	df2	p	lower bound	upper bound
##	Single_raters_absolute	ICC1	0.93	28	19	20	1.9e-10	0.86	0.97
##	Single_random_raters	ICC2	0.93	41	19	19	1.5e-11	0.79	0.97
##	Single_fixed_raters	ICC3	0.95	41	19	19	1.5e-11	0.90	0.98
##	Average_raters_absolute	ICC1k	0.96	28	19	20	1.9e-10	0.92	0.98
##	Average_random_raters	ICC2k	0.96	41	19	19	1.5e-11	0.88	0.99
##	Average_fixed_raters	ICC3k	0.98	41	19	19	1.5e-11	0.95	0.99

**Table 5.5.8: Intra-examiner ICC3 Results for Cleft Side Canine Angulation (Coronal); Investigator LP.** This table displays the intra-examiner intraclass correlation coefficients (ICC3) for cleft side canine angulation in the coronal section. The results are based on initial 20 CBCT images measured by investigator LP. After at least 2 weeks, these same 10 patients (20 CBCT images) were analyzed by investigator LP. An ICC3 value of 0.95 represents excellent

```

## Intraclass correlation coefficients
##
##          type  ICC   F  df1  df2      p  lower bound  upper bound
## Single_raters_absolute  ICC1 0.99 180 19 20 2.7e-18      0.98      0.99
## Single_random_raters    ICC2 0.99 180 19 19 1.6e-17      0.98      0.99
## Single_fixed_raters     ICC3 0.99 180 19 19 1.6e-17      0.98      0.99
## Average_raters_absolute ICC1k 0.99 180 19 20 2.7e-18      0.99      1.00
## Average_random_raters   ICC2k 0.99 180 19 19 1.6e-17      0.99      1.00
## Average_fixed_raters    ICC3k 0.99 180 19 19 1.6e-17      0.99      1.00

```

**Table 5.5.9: Intra-examiner ICC3 Results for Cleft Side Canine Angulation (Sagittal); Investigator LP.** This table displays the intra-examiner intraclass correlation coefficients (ICC3) for cleft side canine angulation in the sagittal section. The results are based on initial 20 CBCT images measured by investigator LP. After at least 2 weeks, these same 10 patients (20 CBCT images) were analyzed by investigator LP. An ICC3 value of 0.99 represents excellent

```

## Intraclass correlation coefficients
##
##          type  ICC   F  df1  df2      p  lower bound  upper bound
## Single_raters_absolute  ICC1 0.99 380 19 20 1.6e-21      0.99      1
## Single_random_raters    ICC2 0.99 458 19 19 2.4e-21      0.99      1
## Single_fixed_raters     ICC3 1.00 458 19 19 2.4e-21      0.99      1
## Average_raters_absolute ICC1k 1.00 380 19 20 1.6e-21      0.99      1
## Average_random_raters   ICC2k 1.00 458 19 19 2.4e-21      0.99      1
## Average_fixed_raters    ICC3k 1.00 458 19 19 2.4e-21      1.00      1

```

**Table 5.5.10: Intra-examiner ICC3 Results for Cleft Side Canine Distance from Occlusal Plane; Investigator LP.** This table displays the intra-examiner intraclass correlation coefficients (ICC3) for cleft side canine distance from the occlusal plane. The results are based on initial 20 CBCT images measured by investigator LP. After at least 2 weeks, these same 10 patients (20 CBCT images) were analyzed by investigator LP. An ICC3 value of 1.0 represents excellent correlation.

## CHAPTER 6: DISCUSSION

### 6.1. Demographic Variables and Their Effects on Outcomes

#### 6.1.1. Gender

There was a statistically significant difference in the volume of the residual defect between males and females ( $F=10.63$ ;  $DF=1,21$ ;  $p=0.0037$ ) in our study. The estimated mean percent residual defect for females was 20.52% (Standard Error = 4.2%) and we are 95% confident the true mean percent residual defect for females is between 13.1% and 30.68%. The estimated mean percent residual defect for males was 44.20% (Standard Error = 5.7%) and we are 95% confident the true mean percent residual defect for males is between 32.93% and 56.1% (Figure 5.2.1.2). These values were compared to and noticeably different than a study by Saruhan and Ertas in 2017. This study used anterior iliac crest as the grafting material for unilateral and bilateral alveolar clefts. They concluded a mean bone fill of 68.23% +/- 9.43% for females and 63.09% +/- 10.72% for males. There was no statistically significant difference found between males and females in this study (Saruhan and Ertas 2017).

It is not likely that a different grafting material, such as rhBMP-2, would cause gender differences to have an effect on alveolar cleft graft outcomes.

#### 6.1.2. Age of the Patient at the Time of Grafting

There was no statistically significant relationship between the percent residual defect and the age of the patient at the time of grafting ( $F=0.00$ ;  $DF=1,21$ ;  $p=0.97$ ). The effect of age on the outcomes of the alveolar bone grafts was calculated as a quantitative/numeric value as well as a qualitative/categorical value. The quantitative/numeric values were reported in our study. Since the data was on the model scale (non-normal data distribution), a direct interpretation could not be determined. However, the direction of the slope value provided insight on how age of the patient at the time of grafting could affect the outcome. The slope value for age and percent

residual defect was -0.00466 and can be seen in Table 5.2.2.2. This negative slope relationship suggests that as age increased within our inclusion criteria range, the percent residual defect decreased and hence bone fill increased.

A systematic review of the literature was completed in 2018 by Kaura et al. to understand how age effects the outcomes of alveolar grafts. When looking at the studies that used chronological age as the determining factor, the authors found the chronological age for alveolar grafting ranged from 10-14 with an average of 10 years old. Our results are similar to the conclusion of this 2018 study; bone grafting completed at an earlier chronologic age did not show better outcomes (Kaura et al. 2018).

### **6.1.3. Side of the Alveolar Cleft**

There was no statistically significant difference in the true mean percent residual defect between left and right side alveolar clefts ( $F=0.6$ ;  $DF=1,21$ ;  $p=0.45$ ). The estimated mean percent residual defect for the left side alveolar cleft was 34.46% (Standard Error = 5.7%) and we are 95% confident the true mean percent residual defect for left side alveolar cleft is between 23.67% and 47.12%. The estimated mean percent residual defect for the right side alveolar cleft was 28.06% (Standard Error = 6.0%) and we are 95% confident the true mean percent residual defect for right side alveolar cleft is between 17.31% and 42.08% (Figure 5.2.3.2).

There is very limited research available on whether the affected side of the patient with unilateral alveolar cleft has an effect on the graft success rate. Our study analyzed this comparison and found no statistically significant difference.

## **6.2. Linear Values and Their Effects on Outcomes**

### **6.2.1. Cleft Side Canine Root Length**

There was no statistically significant relationship between the percent residual defect and length of the canine on the alveolar cleft side ( $F=0.61$ ;  $DF=1,21$ ;  $p=0.44$ ). Since the data was on

the model scale (non-normal data distribution), a direct interpretation could not be determined. However, the direction of the slope value provided insight on how the cleft side canine root length could affect the outcome. The slope value for cleft side canine root length was -0.9491 and can be seen in Table 5.3.1.2. This negative slope relationship suggests that as the length of the canine on the cleft side increased, the percent residual defect decreased and hence bone fill increased.

The overall consensus is that outcomes are better when secondary alveolar bone grafts are completed based on the dental age or root development of the canine on the cleft side. The ideal time for alveolar grafting procedures to be completed is before the eruption of the cleft side canine and when the root of this tooth has one-half to two-thirds of its root development completed (Bergland et al. 1986; Boyne and Sands 1972). In our study, we could not demonstrate a statistically significant difference when analyzing the length of the canine on the cleft side.

### **6.2.2. Cleft Side Canine Angulation; Coronal and Sagittal Sections**

There was no statistically significant relationship between the percent residual defect and the angulation of the canine on the cleft side in neither the coronal section ( $F=2.15$ ;  $DF=1,21$ ;  $p=0.15$ ) nor the sagittal section ( $F=0.13$ ;  $DF=1,21$ ;  $p=0.72$ ). Since the data was on the model scale (non-normal data distribution), a direct interpretation could not be determined. However, the direction of the slope value provided insight on how the angulation of the canine on the cleft side in both the coronal and sagittal sections could affect the outcome. The slope value for the cleft side canine angulation in the coronal section was 0.03561 and can be seen in Table 5.3.2.2. This positive slope relationship suggests that as the angulation, in the coronal section, of the canine on the cleft side increased, the percent residual defect also increased and hence bone fill decreased. The slope value for the angulation of the canine on the cleft side in the sagittal section was -0.00592 and can be seen in Table 5.3.3.2. This negative slope relationship suggests that as

the angulation, in the sagittal section, of the canine on the cleft side increased, the percent residual defect decreased and hence bone fill increased.

Most of the previous studies relating to this variable focuses on the natural eruption of the canine following the secondary alveolar grafting procedure. Vellone et al. studied the effects of secondary alveolar bone grafting on canine eruption. The authors concluded there was no proof that inclination of the canine influenced the eruption before and after the grafting procedure. They did however, conclude secondary alveolar bone grafts significantly affected the natural eruption process of the canine (Vellone et al. 2017). Although this study did not draw a correlation between inclination of the canine and its eruption process, we wanted to understand the effect of canine inclination on overall success rates for unilateral alveolar grafts. It appears that the more upright the permanent canine on the cleft side is, in both sections, at the time of grafting, the higher percentage of bone fill recorded. Still, no statistically significant difference was noticed.

### **6.2.3. Cleft Side Canine Distance from the Occlusal Plane**

There was no statistically significant relationship between the percent residual defect and the distance of the canine on the alveolar cleft side from the occlusal plane ( $F=0.11$ ;  $DF=1,21$ ;  $p=0.74$ ). Since the data was on the model scale (non-normal data distribution), a direct interpretation could not be determined. However, the direction of the slope value provided insight on how the distance of the canine on the cleft side from the occlusal plane could affect the outcome. The slope value for the distance of the canine on the cleft side from the occlusal plane was 0.01404 and can be seen in Table 5.3.4.2. This positive slope relationship suggests that as this distance from the occlusal plane increased, the percent residual defect also increased and hence bone fill decreased.

Our results are similar to those of Upadya et al. This study concluded that the position of the canine on the cleft side, inclination, and distance from the cleft itself, did not have an effect on the success rates of secondary alveolar grafts (Upadya et al. 2013). However, it is still

important to consider the positive slope relationship. It seems as though secondary alveolar grafts can indeed be completed too early in the patients' lives.

### **6.3. Volumetric Values and Percent Residual Defect**

Out of the 24 patients analyzed, one patient was excluded during the statistical analysis with a failed alveolar graft. Data from 23 patients were evaluated for success rates. rhBMP-2 was used for all of the unilateral alveolar cleft grafting procedures completed at the University of Nebraska Medical Center Oral and Maxillofacial Surgery Center. The mean volume of the pre-graft unilateral cleft was  $1026.97\text{mm}^3$  (SD = 390.11) and the mean volume of the post-graft unilateral cleft was  $333.48\text{mm}^3$  (SD = 250.94). These volumes can be seen in Table 5.4.1. The overall average percent residual defect at 6-months post-graft was 0.32 (32%) with a standard deviation of 0.32 (32%). This corresponds to an overall average bone fill of 0.68 (68%) with a standard deviation of 0.22 (22%). These values can be seen in Table 5.4.2.

Our results on the outcomes of secondary grafting unilateral alveolar clefts seem to be slightly lower than previous literature reports. The study by Francis et al. used occlusal radiographs to compare rhBMP-2 and iliac crest as grafting materials. The success rates were 97.2% and 84.2% for rhBMP-2 and iliac crest respectively (Francis et al. 2013). The difference in understanding the pyramid-shaped cleft defect between occlusal radiographs and CBCT images may lead to this difference in results. The 2-dimensional images may overestimate the success rates. Linderup et al. concluded a pre-graft cleft volume of  $934\text{mm}^3$  with an average percentage bone fill of 87%. This study used mandibular symphyseal bone as the grafting material of choice and analyzed the outcomes with CBCT images (Linderup et al. 2016). Oberoi et al. studied the outcomes of secondary bone grafts of alveolar clefts using CBCT images and found an average bone fill of 84% (Oberoi et al. 2009). And finally, a study conducted by Herford et al. specifically focused on the outcomes of repairing the premaxillary cleft using rhBMP-2 and evaluated with CT images found a mean bone fill of 71.7% at 4-months post-graft (Herford et al. 2007).

All of the previous studies mentioned have either used 2-dimensional radiographs to assess a 3-dimensional defect, included unilateral and bilateral alveolar clefts, and/or used a different material to complete the graft procedure. It is important to understand our results using rhBMP-2 to graft unilateral alveolar clefts and evaluating the outcomes using CBCT images. Our results on percent residual defect/percent bone fill are similar to the results reported by Herford et al., which closely resembles our study parameters.

#### **6.4. Limitations of the Study**

##### **6.4.1. Radiographic Limitations**

A limitation of this study is in relation to the method of radiographic capturing, CBCT images. It is well known that CBCT is a reliable tool for orthodontic treatment as well as research modalities (Kapila et al. 2011). However, problems arise when attempting to accurately measure hard tissues, such as the borders of the alveolar cleft defect (Molen 2010). The technology used in this study offers a diagnostic value of 0.2 mm voxels. Theoretically, this means we could measure up to 0.2 mm and be fairly confident at that level. However, previous literature demonstrates that the actual spatial resolution is worse than the true voxel size with factors such as noise and artifact negatively affect the quality of the image (Molen 2010). The spatial resolution used within this study is not entirely known, but past studies of older CBCT images correlated a 0.3 mm voxel size to a spatial resolution around 0.6 mm (Brullmann and Schulze 2015). When trying to understand the amount of percent residual defect or bone fill in the alveolar cleft area, it is important to understand the actual magnitudes of change and assess if they accurately can be measured or assessed based off the voxel size, or more importantly, the true spatial resolution.

CBCT image quality was also a limitation that was noticed during data collection. Medical records and pre-graft/post-graft CBCT images of all patients who received secondary alveolar bone grafts between June 1, 2014 and January 1, 2020 were retrieved. Of the 55 patients



that met our initial criteria, only 24 patients had pre-graft and post-graft CBCT images that were free of noise or artifact.

#### **6.4.2. Software Limitations**

The ITK-SNAP 3.8.0 software used for segmentation introduced other limitations to our study. The degree of image quality and pixelation provided by the software determines the accuracy of measurements. This limitation was observed during the volumetric data gathering process for our unilateral cleft defects. Volumetric segmentation introduced challenges in obtaining a clear distinction between similar grey scale pixels such as those of alveolar bone and grafting material. To overcome these inaccuracies, the volumetric thresholding parameters were set very similar, within ITK-SNAP 3.8.0, when measuring the same patient. Additionally, strict semi-automatic and manual segmentation parameters were developed between the two investigators (LP and SP).

The anterior and posterior borders of the alveolar cleft were determined by manual segmentation. The contralateral normal anatomical bone structure was mimicked to define these borders. The two investigators (LP and SP) were standardized and calibrated before segmentation to eliminate as much subjectivity as possible. Intraclass correlations for inter- and intra-examiner reliability were calculated to determine the accuracy of our measurements. However, this is inevitably a limitation within segmentation studies and has to be mentioned.

Lastly, percent residual defect was reported as our outcome measure to help eliminate the variability within the reported volumetric ranges. This limitation will exist in segmentation research studies until new software updates become available to provide more accurate delineations between grey values that are very similar.

### **6.4.3. Sample Limitations**

Drawing a correlation between our 23 patients included for statistical analysis to the true population is another limitation. Our patients were only sampled from one location, University of Nebraska Medical Center Oral and Maxillofacial Surgery Center. The demographics may not represent the entire population.

Other sample limitations were noted within our study. First, narrowing down patients for our study was dependent on the notes, CBCT images, and histories provided by the oral surgeon at the location mentioned above. We tried to minimize the amount of variability in patient selection by defining specific inclusion and exclusion criteria. Next, true randomization is impossible with the nature of retrospective studies. We attempted to minimize the potential bias during data collection and measurements. Patient records were collected with the specified inclusion and exclusion criteria to reduce bias. Additionally, the 23 patients measured in this study were randomly split up into two groups for the investigators (LP and SP) to segment within ITK-SNAP 3.8.0.

### **6.5. Conclusions**

The present study indicates a statistically significant difference in the percent residual defect exists between males and females. This was the only variable analyzed in this study that demonstrated a significant difference. There was not enough evidence to conclude there is a significant difference in the percent residual defect between left and right side alveolar clefts. Additionally, our data did not demonstrate a significant relationship between the percent residual defect and the following variables: age of the patient at the time of surgery, cleft side canine root length, cleft side canine angulation in the coronal section, cleft side canine angulation in the sagittal section, or cleft side canine distance from the occlusal plane.

Correlation was determined for several of the variables studied. Although not statistically significant, these correlates could provide insight into the relationship that exists between the outcomes of secondary alveolar bone grafts and the variables studied.

The present study also suggests that rhBMP-2 could be an alternative grafting material to anterior iliac crest. With percent residual defect values of 32% and bone fill values of 68% six months following surgery, rhBMP-2 seems to demonstrate similar results compared to other grafting materials. This could allow patients to choose this alternate material to eliminate the complications associated with harvesting anterior iliac crest bone while still achieving successful outcomes.

## **6.6. Future Research**

Future research for this area could address some of the limitations of the present study. The CBCT imaging parameters could be improved to more accurately provide us with the data necessary for research. Spatial resolution and volume rendering software need improvement to allow for more efficient segmentation and to obtain more accurate volumetric data for analysis. Manual segmentation is currently needed during volumetric measurements to distinguish between similar density areas such as alveolar bone and grafting material. The method of calculating a percent residual defect has allowed projects to minimize this effect, but intensive labor is required for manual segmentation. Superior volume segmentation software exists, however most have algorithms that are not verified or standardized. Future studies that use segmentation software that clearly and accurately auto-segments the area of interest would allow for more accurate volumetric parameters and assessments while eliminating the need for tedious manual segmentation.

Our study was retrospective in design with well-defined inclusion and exclusion criteria. Future prospective studies in which records are taken during diagnosis and treatment could provide valuable information. Pre-treatment risk factors could be accounted for if the treatment

protocols were standardized and clinical records were maintained throughout treatment.

Additionally, patient demographics and clinical information such as unilateral or bilateral alveolar cleft, age of the patient, and side of the alveolar cleft could be assessed for treatment standardization.

Finally, a prospective study to compare the outcomes of rhBMP-2 and anterior iliac crest for secondary alveolar bone grafts in unilateral alveolar cleft patients would provide more insight into the effectiveness of this alternative material. A larger sample size, increased variety of patient demographics, and including multiple surgical sites/surgeons may lead to more reliable results when comparing these two grafting materials in a prospective study.

**BIBLIOGRAPHY**

- Amanat N, Langdon JD. 1991. Secondary alveolar bone grafting in clefts of the lip and palate. *J Craniomaxillofac Surg.* 19(1):7-14.
- Bagheri SC, Bell B, Khan HA. 2011. *Current therapy in oral and maxillofacial surgery.* Elsevier Health Sciences.
- Baqain ZH, Anabtawi M, Karaky AA, Malkawi Z. 2009. Morbidity from anterior iliac crest bone harvesting for secondary alveolar bone grafting: An outcome assessment study. *J Oral Maxillofac Surg.* 67(3):570-575.
- Bell WH, Proffit WR, White RP. 1980. *Surgical correction of dentofacial deformities.* Saunders.
- Bergland O, Semb G, Abyholm FE. 1986. Elimination of the residual alveolar cleft by secondary bone grafting and subsequent orthodontic treatment. *Cleft Palate J.* 23(3):175-205.
- Boyne PJ, Sands NR. 1972. Secondary bone grafting of residual alveolar and palatal clefts. *J Oral Surg.* 30(2):87-92.
- Brullmann D, Schulze RK. 2015. Spatial resolution in cbct machines for dental/maxillofacial applications-what do we know today? *Dentomaxillofac Radiol.* 44(1):20140204.
- Chin M, Ng T, Tom WK, Carstens M. 2005. Repair of alveolar clefts with recombinant human bone morphogenetic protein (rhbmp-2) in patients with clefts. *J Craniofac Surg.* 16(5):778-789.
- Cho-Lee GY, García-Díez EM, Nunes RA, Martí-Pagès C, Sieira-Gil R, Rivera-Baró A. 2013. Review of secondary alveolar cleft repair. *Ann Maxillofac Surg.* 3(1):46-50.
- Cobourne MT. 2004. The complex genetics of cleft lip and palate. *Eur J Orthod.* 26(1):7-16.
- Cohen M, Polley JW, Figueroa AA. 1993. Secondary (intermediate) alveolar bone grafting. *Clin Plast Surg.* 20(4):691-705.
- Coots BK. 2012. Alveolar bone grafting: Past, present, and new horizons. *Semin Plast Surg.* 26(4):178-183.
- Craven C, Cole P, Hollier L, Jr., Stal S. 2007. Ensuring success in alveolar bone grafting: A three-dimensional approach. *J Craniofac Surg.* 18(4):855-859.

- Dempf R, Teltzrow T, Kramer FJ, Hausamen JE. 2002. Alveolar bone grafting in patients with complete clefts: A comparative study between secondary and tertiary bone grafting. *Cleft Palate Craniofac J.* 39(1):18-25.
- Dias BDB, Schneider T, Cintra HL. 2018. Platelet-rich fibrin in the alveolar bone graft in cleft lip and palate patient. *International Journal of Growth Factors and Stem Cells in Dentistry.* 1:27.
- Dickinson BP, Ashley RK, Wasson KL, O'Hara C, Gabbay J, Heller JB, Bradley JP. 2008. Reduced morbidity and improved healing with bone morphogenetic protein-2 in older patients with alveolar cleft defects. *Plast Reconstr Surg.* 121(1):209-217.
- Dissaux C, Bodin F, Grollemund B, Bridonneau T, Kauffmann I, Mattern JF, Bruant-Rodier C. 2016. Evaluation of success of alveolar cleft bone graft performed at 5 years versus 10 years of age. *J Craniomaxillofac Surg.* 44(1):21-26.
- Dixon J, Brakebusch C, Fässler R, Dixon MJ. 2000. Increased levels of apoptosis in the prefusion neural folds underlie the craniofacial disorder, treacher collins syndrome. *Hum Mol Genet.* 9(10):1473-1480.
- Eppley BL, van Aalst JA, Robey A, Havlik RJ, Sadove AM. 2005. The spectrum of orofacial clefting. *Plast Reconstr Surg.* 115(7):101e-114e.
- Fahradyan A, Tsuha M, Wolfswinkel EM, Mitchell KS, Hammoudeh JA, Magee W, 3rd. 2019. Optimal timing of secondary alveolar bone grafting: A literature review. *J Oral Maxillofac Surg.* 77(4):843-849.
- Francis CS, Mobin SS, Lypka MA, Rommer E, Yen S, Urata MM, Hammoudeh JA. 2013. Rbmp-2 with a demineralized bone matrix scaffold versus autologous iliac crest bone graft for alveolar cleft reconstruction. *Plast Reconstr Surg.* 131(5):1107-1115.
- Fraser FC. 1970. The genetics of cleft lip and cleft palate. *Am J Hum Genet.* 22(3):336-352.
- Hammoudeh JA, Fahradyan A, Gould DJ, Liang F, Imahiyerobo T, Urbinelli L, Nguyen JT, Magee W, 3rd, Yen S, Urata MM. 2017. A comparative analysis of recombinant human bone morphogenetic protein-2 with a demineralized bone matrix versus iliac crest bone graft for secondary alveolar bone grafts in patients with cleft lip and palate: Review of 501 cases. *Plast Reconstr Surg.* 140(2):318e-325e.
- Herford AS, Boyne PJ, Rawson R, Williams RP. 2007. Bone morphogenetic protein-induced repair of the premaxillary cleft. *J Oral Maxillofac Surg.* 65(11):2136-2141.
- Kang NH. 2017. Current methods for the treatment of alveolar cleft. *Arch Plast Surg.* 44(3):188-193.

- Kapila S, Conley RS, Harrell WE, Jr. 2011. The current status of cone beam computed tomography imaging in orthodontics. *Dentomaxillofac Radiol.* 40(1):24-34.
- Kaura AS, Srinivasa DR, Kasten SJ. 2018. Optimal timing of alveolar cleft bone grafting for maxillary clefts in the cleft palate population. *Journal of Craniofacial Surgery.* 29(6).
- Kazemi A, Stearns JW, Fonseca RJ. 2002. Secondary grafting in the alveolar cleft patient. *Oral Maxillofac Surg Clin North Am.* 14(4):477-490.
- Kim SY, Lim SH, Gang SN, Kim HJ. 2013. Crown and root lengths of incisors, canines, and premolars measured by cone-beam computed tomography in patients with malocclusions. *Korean J Orthod.* 43(6):271-278.
- Lilja J. 2009. Alveolar bone grafting. *Indian J Plast Surg.* 42 Suppl(Suppl):S110-115.
- Linderup BW, Cattaneo PM, Jensen J, Küseler A. 2016. Mandibular symphyseal bone graft for reconstruction of alveolar cleft defects: Volumetric assessment with cone beam computed tomography 1-year postsurgery. *Cleft Palate Craniofac J.* 53(1):64-72.
- Linderup BW, Küseler A, Jensen J, Cattaneo PM. 2015. A novel semiautomatic technique for volumetric assessment of the alveolar bone defect using cone beam computed tomography. *Cleft Palate Craniofac J.* 52(3):e47-55.
- Ludlow JB, Timothy R, Walker C, Hunter R, Benavides E, Samuelson DB, Scheske MJ. 2015. Effective dose of dental cbct-a meta analysis of published data and additional data for nine cbct units. *Dentomaxillofac Radiol.* 44(1):20140197.
- Marazita ML, Mooney MP. 2004. Current concepts in the embryology and genetics of cleft lip and cleft palate. *Clin Plast Surg.* 31(2):125-140.
- Miloro M, Ghali GE, Larsen PE, Waite P, Peterson LJ. 2004. *Peterson's principles of oral and maxillofacial surgery.* BC Decker.
- Molen AD. 2010. Considerations in the use of cone-beam computed tomography for buccal bone measurements. *Am J Orthod Dentofacial Orthop.* 137(4 Suppl):S130-135.
- Oberoi S, Chigurupati R, Gill P, Hoffman WY, Vargervik K. 2009. Volumetric assessment of secondary alveolar bone grafting using cone beam computed tomography. *Cleft Palate Craniofac J.* 46(5):503-511.
- Parker SE, Mai CT, Canfield MA, Rickard R, Wang Y, Meyer RE, Anderson P, Mason CA, Collins JS, Kirby RS et al. 2010. Updated national birth prevalence estimates for selected birth defects in the united states, 2004–2006. *Birth Defects Research Part A: Clinical and Molecular Teratology.* 88(12):1008-1016.

- Proffit WR, Fields HW, Sarver DM. 2013. Contemporary orthodontics. Elsevier/Mosby.
- Rani, Chickmagalur NS. 2011. Classification of cleft lip and cleft palate-a review. *annals and essences of dentistry*. 3:82-94.
- Rawashdeh MA, Telfah H. 2008. Secondary alveolar bone grafting: The dilemma of donor site selection and morbidity. *Br J Oral Maxillofac Surg*. 46(8):665-670.
- S R. 2011. Classification of cleft lip and cleft palate-a review. *annals and essences of dentistry*. 3:82-94.
- Sarkar S, Petiot A, Copp A, Ferretti P, Thorogood P. 2001. Fgf2 promotes skeletogenic differentiation of cranial neural crest cells. *Development (Cambridge, England)*. 128:2143-2152.
- Saruhan N, Ertaş U. 2017. The evaluation of gender effect in treatment of alveolar cleft with iliac bone graft by means of volumetric analysis. *Middle Black Sea Journal of Health Science*. 3:16-16.
- Schutte BC, Murray JC. 1999. The many faces and factors of orofacial clefts. *Hum Mol Genet*. 8(10):1853-1859.
- Seifeldin SA. 2016. Is alveolar cleft reconstruction still controversial? (review of literature). *Saudi Dent J*. 28(1):3-11.
- Shrout PE, Fleiss JL. 1979. Intraclass correlations: Uses in assessing rater reliability. *Psychol Bull*. 86(2):420-428.
- Snead MP, Yates JR. 1999. Clinical and molecular genetics of stickler syndrome. *J Med Genet*. 36(5):353-359.
- Sperber GH, Geoffrey H, Sperber GDGMS, Wald J, Gutterman GD, Sperber SM. 2001. Craniofacial development (book for windows & macintosh). B C Decker.
- Stoelinga PJW, Haers PEJJ, Leenen RJ, Soubry RJ, Blijdorp PA, Schoenaers JHA. 1990. Late management of secondarily grafted clefts. *International Journal of Oral and Maxillofacial Surgery*. 19(2):97-102.
- Tolarová MM, Cervenka J. 1998. Classification and birth prevalence of orofacial clefts. *Am J Med Genet*. 75(2):126-137.
- Trindade IK, Mazzottini R, Silva Filho OG, Trindade IE, Deboni MC. 2005. Long-term radiographic assessment of secondary alveolar bone grafting outcomes in patients with alveolar clefts. *Oral Surg Oral Med Oral Pathol Oral Radiol Endod*. 100(3):271-277.



- Upadya VH, Bhat HHK, Gopalkrishnan K. 2013. Radiographic assessment of influence of cleft width and canine position on alveolar bone graft success: A retrospective study. *J Maxillofac Oral Surg.* 12(1):68-72.
- van Aalst JA, Kolappa KK, Sadove M. 2008. Moc-pssm cme article: Nonsyndromic cleft palate. *Plast Reconstr Surg.* 121(1 Suppl):1-14.
- van Hout WM, Mink van der Molen AB, Breugem CC, Koole R, Van Cann EM. 2011. Reconstruction of the alveolar cleft: Can growth factor-aided tissue engineering replace autologous bone grafting? A literature review and systematic review of results obtained with bone morphogenetic protein-2. *Clin Oral Investig.* 15(3):297-303.
- Vellone V, Cirignaco G, Cavarretta B, Cascone P. 2017. Canine eruption after secondary alveolar bone graft in unilateral cleft lip and palate patients. *The Journal of craniofacial surgery.* 28(5):1206-1210.
- Venkatesh R. 2009. Syndromes and anomalies associated with cleft. *Indian J Plast Surg.* 42 Suppl(Suppl):S51-55.